Flexural design of precast, prestressed ultra-high-performance concrete members

Chungwook Sim, Maher Tadros, David Gee, and Micheal Asaad

- This paper proposes flexural design recommendations for precast, pretensioned ultra-high-performance concrete members, including experimental verification and numerical examples. The experimental program includes three examples: a precast, prestressed concrete decked I-beam; a precast, prestressed concrete floor slab; and a precast, prestressed concrete bridge box beam. A comprehensive design example of a 250 ft (76.2 m) long decked I-beam is presented. A design spreadsheet is available online to aid designers in implementing the proposed recommendations.
- For the purposes of this research, less emphasis is placed on the ultra-high-performance concrete achieving extremely high compressive strength, which does not appear to be economically justifiable, and more emphasis is placed on the tensile properties that allow for significant reduction of secondary and shear reinforcement while still achieving excellent durability behavior.
- The use of ultra-high-performance concrete for main structural members can be attractive for both building and bridge applications by achieving optimized, cost-effective cross sections.

PCI Journal (ISSN 0887-9672) V. 65, No. 6, November–December 2020.

PCI Journal is published bimonthly by the Precast/Prestressed Concrete Institute, 8770 W. Bryn Mawr Ave., Suite 1150, Chicago, IL 60631.

This paper is based on research performed for PCI in the project "Implementation of Ultra-high-performance Concrete in Long-Span Precast, Pretensioned Elements for Concrete Buildings and Bridges." Phase I of the project reported on the development of mixtures with focus on quality control procedures and cost analysis for six precast concrete companies.[1] The phase I report shows that mixtures produced and mixed in conventional precast concrete plants can provide ultra-high-performance concrete (UHPC) with the properties specified for the project at a fraction of the cost of prebagged materials available in the U.S. market. An example of a mixture used by one of the precast concrete companies consisted, per cubic yard (per cubic meter), of 1297 lb (588 kg) of Type I/II cement, 324 lb (147 kg) of silica fume, 143 lb (65 kg) of limestone powder, 1881 lb (853 kg) of fine (masonry) sand, 288 lb (131 kg) of water, and high-range water-reducing admixture and workability admixture as needed to achieve flow of 8 to 10 in. (203 to 254 mm). In addition, 264 lb (120 kg) of 0.0079 in. (0.2 mm) diameter × 0.47 in. (12 mm) long steel fibers with a strength of 362 ksi (2500 MPa) were added. This corresponded to 2% fractional volume of the mixture. Before the mixture was tried in the plant, lab testing of heat-cured 2 × 2 in. (51 × 51 mm) cubes produced a 28-day strength of 26 ksi (179 MPa). The same mixture was produced in a precast concrete plant and was not subjected to any curing. It produced properties meeting all the requirements listed in the next section, except that the cylinder compressive strength was 17.9 ksi (123 MPa), which was less than 18 ksi (124 MPa). Applying heat curing as recommended for

UHPC would have resulted in significantly higher compressive strength.

The phase I report[1] also indicated that it is possible, with the conservative tentative recommendations, for structural design to optimize the product shapes to have nearly 50% of the weight of conventional members and to nearly eliminate the need for reinforcing bars. The combination of lower material unit cost and lower product weight allows for cost-competitive design based on the structural criteria alone. When increased service life and other factors, such as lower product transportation cost, reduced foundation, and reduced shoring, are considered, the use of UHPC in main structural members becomes even more attractive.

The PCI project has a unique definition of UHPC, which is referred to in this paper as PCI-UHPC. This definition places less emphasis on achieving extremely high, and currently underused, compressive strength, in the range of 21.7 to 29 ksi (150 to 200 MPa) and more emphasis on the considerably higher-impact tensile properties that allow for a significant reduction of secondary and shear reinforcement. The minimum properties of PCI-UHPC still achieve outstanding durability behavior.

Minimum required properties of UHPC

For structural design purposes, PCI-UHPC must meet the following minimum requirements, with specimens prepared and tested according to the general requirements of ASTM C1856[2] for UHPC:

- Compressive strength, according to ASTM C39,[3] at prestress release = 10 ksi (69 MPa).
- Compressive strength, according to ASTM C39,[3] at service (either 28 days or 56 days, as defined by the structural engineer) = 18 ksi (124 MPa).
- Flexural tension stress, according to ASTM C1609,[4] which is based on linear uncracked stress analysis, must meet the following minimum requirements: minimum first peak (cracking) stress = 1.5 ksi (10 MPa); minimum peak stress = 2.0 ksi (14 MPa); minimum peak-to-first peak (cracking) stress ratio = 1.25, which is a measure of strain hardening; minimum stress at deflection of (L/150)/cracking stress = 0.75, which is a measure of ductility, where L is the span length of the test prism. These requirements were adopted in part from section 26.12.5 of the American Concrete Institute's *Building Code Requirements for Structural Concrete (ACI 318-19) and Commentary (ACI 318R-19)*[5] to ensure strain hardening and ductile behavior.
- Resistance to chloride ion penetration, according to ASTM C1202,[6] ≤500 coulombs for structures exposed to chlorides. Note that this test is performed on specimens without steel fibers.

In addition to these properties, it is assumed in this paper that the modulus of elasticity of concrete can be taken as 5000 ksi (34,500 MPa) at time of release of pretension and 6500 ksi (44,800 MPa) at service. Further, the prestress losses are simplified as 10% of the initial tension of the strands at prestress release and 20% at final time. Further research is needed to refine these values; however, further refinements may result in little or no savings in the number of strands required. For the purpose of estimating camber, long-term creep at the time of member erection is assumed to equal 1.0. Experience gained in actual construction with PCI-UHPC may require further tweaking for the estimation of the creep coefficient. Long-term camber variability is recognized in the decked I-beam example given in this paper by allowing for use of adjustable top nonbonded post-tensioning strands.

Structural modeling of tensile properties

Figure 1 shows a sampling of the results of the ASTM C1609[4] testing of UHPC concrete mixed in the six precast concrete plants that participated in the PCI study. For example, for one of the mixtures, cracking stress = 2.19 ksi (15 MPa) > 1.5 ksi (10 MPa) and peak stress = 3.62 ksi (25 MPa) > 2 ksi (14 MPa). The peak stress–to–cracking stress ratio = 1.65 > 1.25, and the ratio of stress at L/150 to cracking stress = 1.29 > 0.75. Thus, all strength, strain hardening, and ductility requirements were met.

Figure 2 is a representation of information in Fig. 1 with stress converted to midspan moment and deflection converted to midspan curvature. Figure 2 also shows the minimum values used in structural design, starting with the first peak (cracking) stress set at 1.5 ksi (10 MPa). The other parameters were conversions from that minimum required cracking stress, not the actual cracking stress, as required for qualifying the mixture proportions. This conservative approach adds further safety margins to the design. Converting the load in the ASTM C1609[4] test to the midspan moment is straightforward. The moment = PL/6, where P is the applied load, placed at the third points.

Converting midspan deflection to midspan curvature employs the theory of elasticity relationship that curvature is the second derivative of deflection. Assume, as a practical approximation, that the curvature diagram is parabolic. Double integration of curvature to obtain deflection is analogous to double integration of distributed load to get moment. The distributed load here is not a typical uniform load, but it follows a second-degree parabola. Recognizing the geometric properties of parabolas, the analogous midspan moment due to this load can be determined by simple equilibrium analysis of a free-body diagram representing one half of the span. It can be shown to result in a midspan curvature-to-deflection relationship of $48/5L^2$. The plots in Fig. 2 are further simplified by connecting the important points with straight lines. Figure 2 clearly shows that the values specified for structural design are significantly below the average values from testing. This conservative approach is believed to be justified at this time

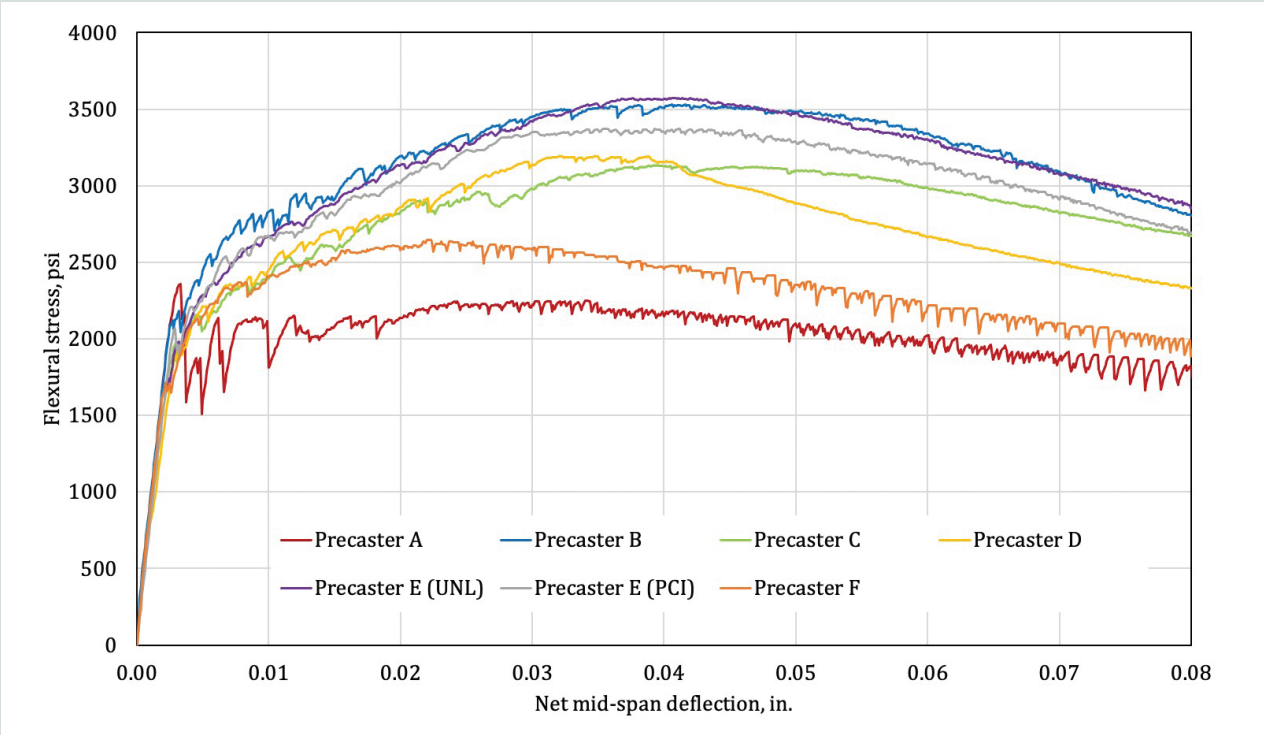

Figure 1. ASTM C1609 flexural stress versus deflection diagrams for six precast concrete manufacturers from average of three specimens each. Note: UNL = UHPC mixture developed by the University of Nebraska–Lincoln; PCI = UHPC mixture developed per the phase I report; UHPC = ultra-high-performance concrete. 1 in. = 25.4 mm; 1 psi = 6.895 kPa.

and until more data are accumulated on the tensile behavior of PCI-UHPC.

For establishing tensile properties of UHPC, some researchers, such as Reineck and Frettlöhr[7] and Graybeal and Baby,[8] have proposed uniaxial tensile testing methods; however, these methods are nonstandard, highly variable, and not easily repeatable. The testing specimens and apparatus are only available in a few research labs and are not easily accessible to commercial producers in the United States. Furthermore, neither uniaxial nor prism testing is an exact replication of the stress field that exists in the webs of flexural members. This is analogous to accepting the fact that cylinder testing in compression is not an exact replication of compressive strength in the bottom flange of an I-beam. Accordingly, the method recommended here for tensile properties is ASTM C1609[4] prism testing. López and colleagues[9] and codes and guidelines from other nations—for example, France,[10] Switzerland,[11] Germany,[12] and Canada[13]—support this recommendation.

One disadvantage of testing according to ASTM C1609[4] is that the stresses are nominal values calculated from the measured load and converted to flexure and then to stress using linear elastic analysis, even at peak loading and beyond, where the material properties become nonlinear. The stress representing initiation of flexural cracks is theoretically correct. This is the value required here to be ≥1.5 ksi (10 MPa). However, beyond cracking, adjustments that are called *inversion* in the literature must be made to allow for the use of the test results in structural design for ultimate loading effects. As presented in the next section, methods of deriving the allowable capacity at factored load effects can be used in spreadsheet analysis. Alternatively, some international guides have allowed using a factor of about 0.3 to 0.4 of the nominal stress at peak load as the available residual maximum strength on the tension side of the neutral axis of a flexural member.

One of the goals of this research is to develop a conservative design procedure that accounts for the presence of the fibers in enhancing the flexural capacity of bridge and building products. To achieve this goal, the characteristics of the concrete in tension, represented by Fig. 2, must be idealized into a designer-friendly model. For the service limit state, it is relatively simple to calculate the stress using a linear elastic uncracked concrete section. The resulting tensile stress would need to be less than 1.5 ksi (10 MPa) to indicate no cracking under service load. A factor of safety is proposed to be introduced here to limit the extreme fiber tensile stress to 1.0 ksi (7 MPa) to ensure a margin against cracking. The same factor is used for members reinforced with prestressed strands as for members reinforced with nonprestressed bars.

For the strength limit state, the moment capacity of the cross section should be less than that corresponding to 2.0 ksi

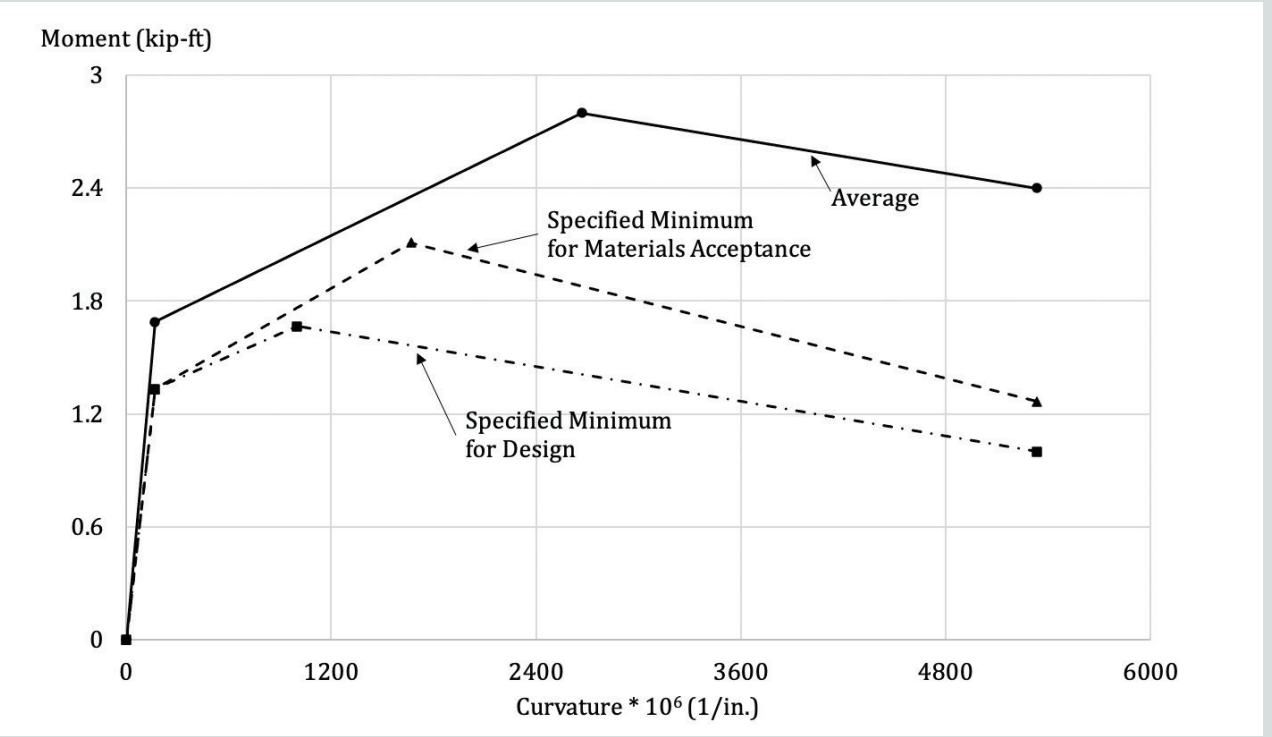

Figure 2. Average observed flexural stress from six precast concrete manufacturers compared with minimum recommended properties. Note: 1 in. = 25.4 mm; 1 kip-ft = 1.356 kN-m.

(14 MPa) peak stress in the ASTM C1609[4] testing, which corresponds to the peak point given in Fig. 2 on the specified minimum for design curve. To obtain a satisfactory solution, strain compatibility analysis—known as inverse analysis—must be conducted. For the inverse analysis to be performed, the stress-strain relationship in flexural tension must be first assumed and iteratively refined. Multiple studies have been performed using various models of the stress-strain relationship.

Figure 3 shows an idealization of the stress-strain relationship of UHPC in compression and in tension.[14] The tensile stress-strain relationship is expressed as trilinear. The values of first-peak flexural stress using linear stress analysis f_{fc} = 1.50 ksi (10 MPa) and $\frac{5}{8}f_{fc}$ = 0.94 ksi (6 MPa) results in strains at the end of the first linear segment of 0.000144. The strain at the end of the horizontal line is $0.16L_f/1.2h$ = $(0.16)(0.75)/1.2h = 0.1h$, with a limit of 0.004, where L_f is the fiber length and h is the depth of the member, both in inches. The total strain limit at the end of the descending line (at zero stress) is set at $L_f/1.2h = 0.625/h$ and is not greater than 0.01. Gowripalan and Gilbert[14] proposed that for concrete members reinforced exclusively with fibers in flexure, the flexural capacity be determined based on extreme fiber tensile strain not exceeding either $0.16L_f/1.2h$ or 0.004.

Graybeal[15] evaluated the structural behavior of prestressed UHPC I-girders. **Figure 4** shows the proposed stress-strain response in tension and compression.[16] Graybeal's simplified stress-strain response was considered conservative compared with flexural strength experiments. The ultimate compressive stress and strain were limited to $0.85f'_c$ and 0.0035, respectively, where f'_c = compressive strength of concrete. The ultimate tensile stress and strain were limited to 1.50 ksi (10 MPa) and 0.007, respectively.

When Vande Voort and coauthors[17] investigated the behavior of UHPC for piles, they modeled the tensile stress-strain relationship, setting the modulus of elasticity to 8000 ksi (55,200 MPa), cracking strength to 1.30 ksi (9.0 MPa), and peak tensile strength to 1.70 ksi (11.7 MPa).

Fehling and Leutbecher[18] proposed the stress-strain relationship shown in **Fig. 5**. They proposed a rectangular stress block in the bottom 90% of the tension zone, with the linear distribution ignored. They also proposed an average stress of 0.85 to 0.90 of the tensile strength, with the lower ratio used for tee beam sections.

Naaman[19] performed a numerical investigation of the effects of various shapes of stress-strain diagrams on the flexural resistance of fiber-reinforced concrete without longitudinal reinforcement. The tensile stress diagram is represented by a rectangle for strain-hardening mixtures and a triangle for strain-softening mixtures. The flexural tensile strength is assumed equal to the average tensile stress in uniaxial testing. The strain-softening model was shown to cause the moment

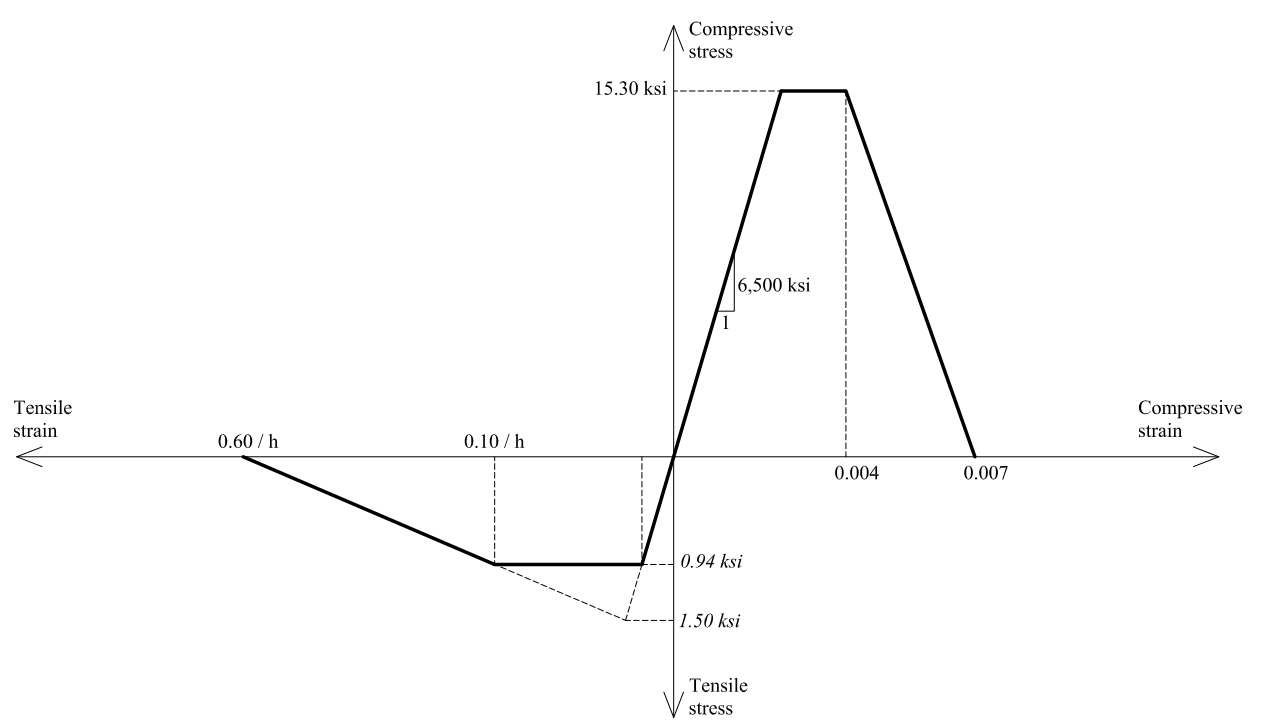

Figure 3. Idealized stress-strain relation in compression and tension. Source: Adapted from Gowripalan and Gilbert (2000, Fig. 2 and 5). Note: *h* = overall thickness or depth of a member. 1 ksi = 6.895 MPa.

capacity to be reduced by as much as 28%. Note that the authors of this paper did not allow the use of mixtures with strain softening.

International codes tend to assume nonlinear stress-strain relationships with critical points defined by testing and with safety factors introduced to material properties, rather than to total internal forces as is customary in both ACI 318[5] and the American Association of State Highway and Transportation Officials' *AASHTO LRFD Bridge Design Specifications*. An example is represented by **Fig. 6** from the Japanese Society of Civil Engineers.[21] The first line has a slope of the modulus of elasticity until reaching first-crack tensile strength. The strain is then increased by increasing the stress until the postcracking tensile strength and the ultimate strain limit are reached. The Korea Concrete Institute's *Guidelines for K-UHPC Structural Design*[22] also use a bilinear relationship for UHPC with tensile strain hardening.

Annex 8.1 of the *Canadian Highway Bridge Design Code*[13] specifies design guidelines for fiber-reinforced concrete in general, not UHPC specifically. The moment-curvature response given by Gowripalan and Gilbert[14] was adopted in the Canadian code. For primary load-bearing members, the contribution of the fibers is limited, per annex 8.1 of the Canadian code, to a maximum of 20% of the factored moment demand. For secondary members, reinforcing bars may be eliminated if the factored moment demand does not exceed 50% of the flexural resistance.

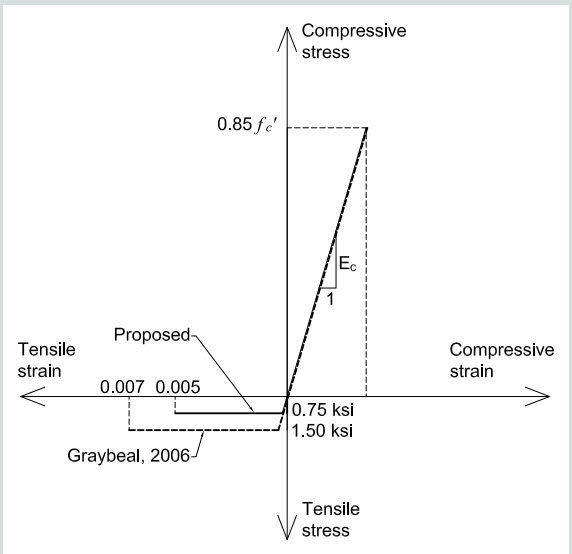

Figure 4. Stress-strain behavior for flexural design compared to that by Graybeal. Source: Adapted from Graybeal (2006, Fig. 77). Note: E_c = modulus of elasticity of concrete; f'_c = compressive strength of concrete. 1 ksi = 6.895 MPa.

Modeling of the stress-strain diagram in compression is relatively simple. Historically, in the 70 years since the introduction of the strength design method in U.S. codes, the equivalent rectangular stress block with a unit stress of $0.85 f'_c$ and a depth

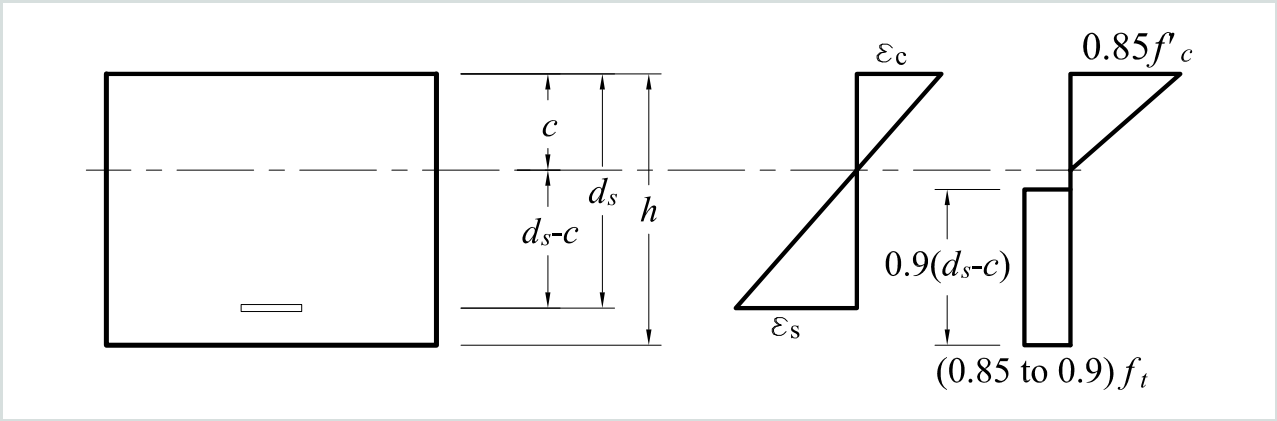

Figure 5. Model for design for flexural strength, according to Fehling and Leutbecher. Source: Adapted from Fehling et al., *Ultra-High Performance Concrete* (Berlin, Germany: Ernst & Sohn, 2014), Fig. 5.7. Note: c = distance from the extreme compression fiber to the neutral axis; d_s = distance from extreme compression fiber to the centroid of the nonprestressed tensile reinforcement measured along the centerline of the web; f'_c = compressive strength of concrete; f_t = tensile stress corresponding to certain loads during uniaxial tensile tests; h = overall thickness or depth of a member; ε_c = strain of concrete in extreme compressed fiber; ε_s = strain in the reinforcement.

equaling the product of the stress factor β_1 multiplied by the neutral axis depth has worked very well. In this relationship, β_1 varies from 0.85 for $f'_c \le 4$ ksi (28 MPa) to 0.65 for $f'_c \ge 8$ ksi (55 MPa). Rizkalla and colleagues[23] showed that for concrete strengths from 10.0 to 18.0 ksi (69 to 124 MPa), the assumption of $\beta_1 = 0.65$ is still valid. The 0.65 value recognizes the fact that the actual cylinder stress-strain relationship tends to be close to a straight line and a triangular stress distribution would have a center of force at $c/3$ from the top fibers, the same as that for the equivalent rectangular stress block, where c = distance to the neutral axis. As recently as 2017, Naaman[19] also confirmed the insensitivity of nominal moment to variations of the assumed shape of the compression stress block. Other shapes are proposed by Gowripalan and Gilbert,[14] Graybeal,[16] Vande Voort and coauthors,[17] Fehling and Leutbecher,[18] and Naaman[19] (Fig. 3–5).

In this paper, the equivalent rectangular stress block will be assumed in obtaining the nominal strength of PCI-UHPC members at an extreme fiber strain of 0.003. In addition, the model used by Graybeal[16] will be adopted, except that tensile stress at a strain greater than 0.005 will be taken to equal zero and the maximum stress is calculated through inverse analysis as shown in the following section. The final value of flexural capacity will be the higher of that obtained from ultimate strain analysis and from the nonlinear modified Graybeal model. As will be shown later in this paper, the maximum moment of prestressed members is controlled by the ultimate strain and rectangular stress block analysis in most cases. In the design of members without prestressing (for example, the transverse direction of a box or decked I-beam), either method can produce the maximum design capacity.

Inverse analysis

López and coauthors[24] developed a model for conversion of the ASTM C1609[4] prism testing results into nonlinear

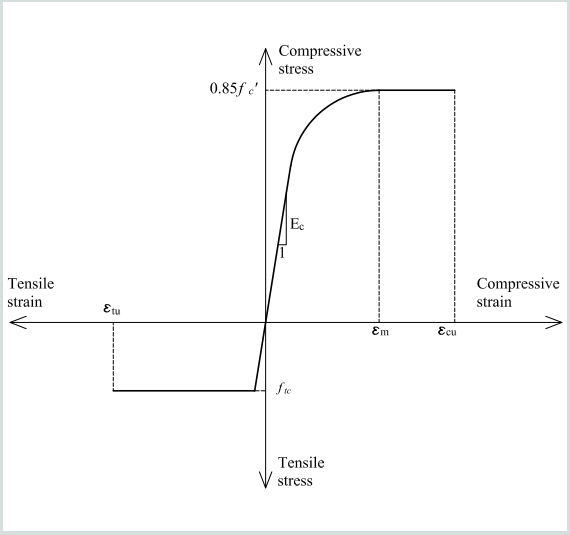

Figure 6. Idealized stress-strain relation in compression and tension according to the Japan Society of Civil Engineers. Source: Adapted from the Japan Society of Civil Engineers (2008, Fig. 3.3.1 and 3.3.2). Note: E_c = modulus of elasticity of ultra-high-performance concrete; f'_c = compressive strength of concrete; f_t = tensile stress corresponding to certain loads during uniaxial tensile tests; f_{tc} = first-peak (cracking) stress using uniaxial tensile tests; h = overall thickness or depth of a member; ε_{cu} = failure strain of concrete in compression; ε_m = compressive strain at peak compressive stress; ε_{tu} = design failure strain of concrete in tension.

stress-strain relationships at various levels of loading beyond cracking. The procedure is known as inverse analysis and has recently been adopted in the Canadian standards.[13] In this paper, the tensile stress-strain relationship is assumed to be a simple bilinear curve, as previously discussed. The compressive stress-strain relationship is assumed to be linear elastic

up to stress = $0.85f'_c$. Figure 4 represents both sides of the neutral axis. To further simplify the iterative analysis performed here, the tensile stress diagram is reduced to zero at a strain greater than 0.005. The goal of the analysis is to obtain the most accurate value of the tensile stress f_{fe} in place of the 1.5 ksi (10 MPa) proposed by Graybeal[25] to represent the PCI-UHPC material properties stated earlier. The 0.005 strain is conservative and consistent with the recommendations of Naaman and Reinhardt.[26]

Figure 2 provides the average and minimum stress requirements in prism testing according to ASTM C1609.[4] These stresses, as indicated earlier, are nominal values calculated using linear uncracked section analysis of the 4 × 4 × 14 in. (100 × 100 × 350 mm) standard test prism. The following steps are used iteratively to obtain the value of f_{fe} that produces the maximum moment in a diagram constructed using specified minimum values to be used in structural design.

To develop the moment-curvature relationship, a value of f_{fe} is initially assumed. Each point on the curve is obtained by following these steps:

1. Select a value of the strain of concrete at the extreme compression fiber ε_c.
2. Assume neutral axis depth c, and develop the strain diagram across the full depth.
3. Using the stress distribution in Fig. 4, calculate the stresses and forces. If the sum of forces equals zero, pure bending has been achieved. If not, repeat steps 1 and 2 until equilibrium is reached.
4. Calculate the moment, and plot it versus the corresponding curvature as one point on the moment-curvature curve.
5. Repeat steps 1 through 4 to create the full moment-curvature diagram for a given value of f_{fe}.
6. Repeat the process to create curves for different values of f_{fe}.
7. Assume that the useful zone for design is limited to an extreme tensile strain of 0.005. Select the value of f_{fe} that most closely represents the values given by the specified minimum for design.

As shown in **Fig. 7**, a value of f_{fe} = 0.75 ksi (5.2 MPa) represents a reasonably accurate limit for nonlinear flexural analysis beyond cracking. Please note that the value of nominal flexural resistance M_n = 1.67 kip-ft (2.26 kN-m) is the theoretical nominal strength according to the proposed stress-strain model in Fig. 4. It is interesting to note that using linear elastic uncracked analysis, the minimum peak tensile stress required for PCI-UHPC products is 2 ksi (13.8 MPa). This stress corresponds to a peak load moment that equals the product of 2 ksi multiplied by the section modulus of the 4 × 4 in. (100 × 100 mm) prism or 1.78 kip-ft (2.41 kN-m). This is a good confirmation of the accuracy of the results of the inverse analysis given here.

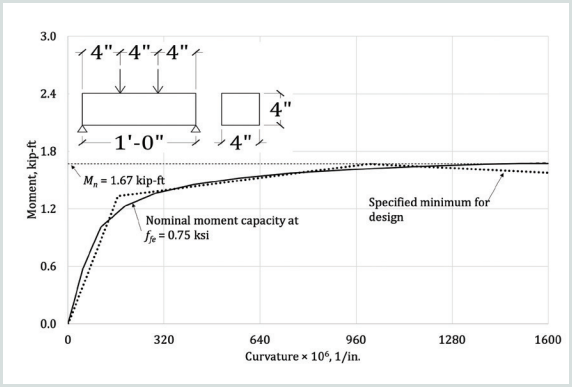

Figure 7. Comparison of specified minimum equivalent bilinear strength according to ASTM C1609 and theoretical moment-curvature diagram using the stress-strain model in Fig. 4 with equivalent bilinear strength of 0.75 ksi. Note: f_{fe} = equivalent bilinear strength to the linear peak stress obtained by ASTM C1609; M_n = nominal flexural resistance. 1″ = 1 in. = 25.4 mm; 1′ = 1 ft = 0.305 m; 1 kip-ft = 1.356 kN-m.

Proposed design criteria

The following design criteria are proposed to be used in the flexural design of UHPC members. The criteria are valid regardless of whether reinforcing bars or prestressing strands are used. They are valid for both building and bridge products. The resistance factors used in the proposal should be the same as those used in ACI 318[5] for buildings or in the AASHTO LRFD specifications[20] for bridges. One exception is related to resistance factors when fibers are used to contribute to flexural strength. For this case, a formula for resistance factor gradually transitioning from total dependence on fibers to zero dependence on fibers to resist the applied moments was developed and is shown in the strength reduction factor section.

Service limit state

For the concrete complying with the minimum criteria specified for PCI-UHPC, the maximum allowable tensile stress for both reinforced and prestressed concrete is recommended to be 1.00 ksi (7 MPa) at service. The corresponding limit at prestress release is 0.75 ksi (5 MPa), which is approximately the ratio of $\sqrt{\frac{f'_{ci}}{f'_c}} = \sqrt{\frac{10}{18}}$, where f'_{ci} = required concrete compressive strength at transfer. If a nonprestressed member is supplied with reinforcing bars and is not limited to fibers only, it is permissible to design a cracked member according to prevailing methods from ACI 318[5] and the AASHTO LRFD specifications[20] with the fibers ignored in crack-control calculations. The

authors realize that this recommendation is quite restrictive. Further research may allow for its relaxation in the future.

Strength limit state

Reinforcement may be provided in several of forms: fibers, mild steel bars, high-strength steel bars, and prestressing strands. For mild steel, Grade 60 (414 MPa) meeting ASTM A615[27] requirements, an elastic and perfectly plastic stress-strain diagram is generally accepted in design. Due to the relatively thin members used with UHPC, and for closer compatibility with the high concrete strength, it is recommended that ASTM A1035[28] Grade 100 (690 MPa) steel be used. For that steel, the ACI Innovation Task Group (ITG) 6-10,[29] recommends a stress-strain diagram using Eq. (1), (2), and (3), as follows:

$$f_s = 29{,}000\varepsilon_s \text{ ksi for } \varepsilon_s \le 0.0024 \quad (1)$$

$$f_s = 170 - \frac{0.43}{\varepsilon_s + 0.0019} \text{ ksi for } 0.0024 < \varepsilon_s \le 0.02 \quad (2)$$

$$f_s = 150 \text{ ksi for } 0.02 < \varepsilon_s \le 0.06 \quad (3)$$

where

f_s = allowable stress in steel

ε_s = strain in reinforcement

According to Devalapura and Tadros,[30] a best fit of the lower bound of the experimental results for the nonlinear stress-strain relationship of high-strength bars and strands can be obtained through the use of the power formula shown in Eq. (4).

$$f_s = E_s\varepsilon_s\left[Q + \frac{1-Q}{\left[1+\left(\frac{E_s\varepsilon_s}{Kf_{py}}\right)^R\right]^{\frac{1}{R}}}\right] \le f_{su} \quad (4)$$

where

E_s = the modulus of elasticity of the steel

Q = curve-fitting coefficient

K = curve-fitting coefficient

f_{py} = yield strength of prestressing steel

R = curve-fitting coefficient

f_{su} = specified tensile strength of the steel

These values are E_s = 29,000 ksi (199,955 MPa), Q = 0.035, K = 1.02, R = 2.042, and f_{su} = 150 ksi (1034 MPa) for ASTM A1035[28] bars. The corresponding values for ASTM A416[31] Grade 270 (1862 MPa) low-relaxation strands are E_s = 28,500 ksi (196,501 MPa), Q = 0.031, K = 1.04, R = 7.36; and f_{su} = 270 ksi (1860 MPa).

The power formula shown in Eq. (4) has already been adopted in the *PCI Bridge Design Manual*[32] and in commercial software. It produces nearly identical results to the ACI ITG 6-10[29] formulas for ASTM A1035[28] steel. Because it is only one relationship, it can more easily be programmed in spreadsheet calculations than the three formulas in the ACI ITG 6-10 and other models.

For concrete mixtures meeting the minimum PCI-UHPC properties, flexural strength is to be calculated as the larger of two values, as shown in the following two options:

1. Use the tension and compression stress-strain diagrams recommended in Fig. 4 with the values derived in this research. This model allows for construction of the full moment-curvature diagram for given cross-section dimensions and reinforcement. Establish the peak value of moment on the curve.

2. Use the conventional equivalent rectangular stress block on the compression side of the neutral axis with the extreme compressive strain of 0.003 and the tension model adopted in option 1. Establish the nominal resistance that satisfies equilibrium and strain compatibility as is traditionally done with conventional concrete.

The larger of the two moments from options 1 and 2 will be the flexural strength of the section.

As will be shown in parametric studies and examples, the strength from option 2 will be the controlling value unless very light prestress is provided. It will also be shown that ignoring the fibers in option 2 would result in an insignificant loss of flexural capacity; however, there may be cases where prestressing is very low and the designer wishes to take advantage of the contribution of the fibers.

A workbook developed by the authors is offered in a spreadsheet that includes both options 1 and 2. It can be found online at https://www.pci.org/2020Nov-Workbook.

Strength reduction (resistance) factor in flexure

Almost all of the factors already specified in ACI 318[5] and the AASHTO LRFD specifications[20] are recommended to be adopted at this time; however, there is one exception. It is recognized that for members reinforced with fibers alone, there is a shortage of research data to justify considering the flexural behavior to be ductile. There is concern that once fibers pull out of one side across a formed crack, the member will split into two pieces without adequate warning. It is therefore recommended that the resistance factor for moment ϕ corresponding to compression-controlled behavior be applied to the contribution of fibers to the flexural capacity

of the section being considered. This factor, called resistance for compression-controlled members ϕ_{cc}, is 0.65 in ACI 318[5] and 0.75 in the AASHTO LRFD specifications.[26] The value of resistance for tension-controlled members ϕ_{tc} for tension-controlled behavior is different for building members than for bridge members. It is proposed that the respective value for the member being designed be used.

It is recommended that the resistance factor ϕ be determined in two steps:

1. Calculate the resistance factor when the fiber contribution is ignored ϕ_b in accordance with the respective code based on tension-controlled, compression-controlled, or transition conditions with the fiber contribution ignored.

2. Calculate the final ϕ value according to Eq. (5):

$$\phi = \phi_{cc} + 0.30\left(\frac{M_{nb}}{M_n}\right) \le \phi_b \quad (5)$$

where

M_{nb} = nominal flexural resistance of flexural reinforcement only, ignoring fiber contribution

$\frac{M_{nb}}{M_n}$ = the ratio of the contribution of the longitudinal continuous reinforcement (bars or strands) to the total nominal moment

For example, for a building member section with no bars or strands, the ϕ value would be 0.65. If bars or strands contribute 90% of the total capacity, the ϕ value = 0.65 + (0.3 × 0.9) = 0.92; however, the upper limit, the 0.90 resistance factor with fibers ignored, would control. Similarly, with bars and/or strands providing 60% of the total capacity, the value of ϕ is either 0.65 + (0.3 × 0.6) = 0.83 or the value of ϕ_b based on analysis with fibers ignored, whichever is lower. For prestressed members, it is very likely, as previously described, that the value of ϕ will be calculated to be the typical 0.9 in buildings and 1.0 in bridges.

Evaluation of contributing parameters to flexural strength

Contribution of fibers in prestressed members

The decked I-beam being used as one of the recommended products in this research is used here to investigate the contributions of the various components of the section to the flexural strength of the midspan section of the member. **Figure 8** shows the cross section of a decked I-beam at midspan and the nominal moment capacity as the number of strands increases in the bottom flange of the cross section.

The inset figures show the moment-curvature relationship obtained by using the online spreadsheet. It can be seen that members with very few strands experience peak capacity due to the fiber contribution; however, that peak is not sustained

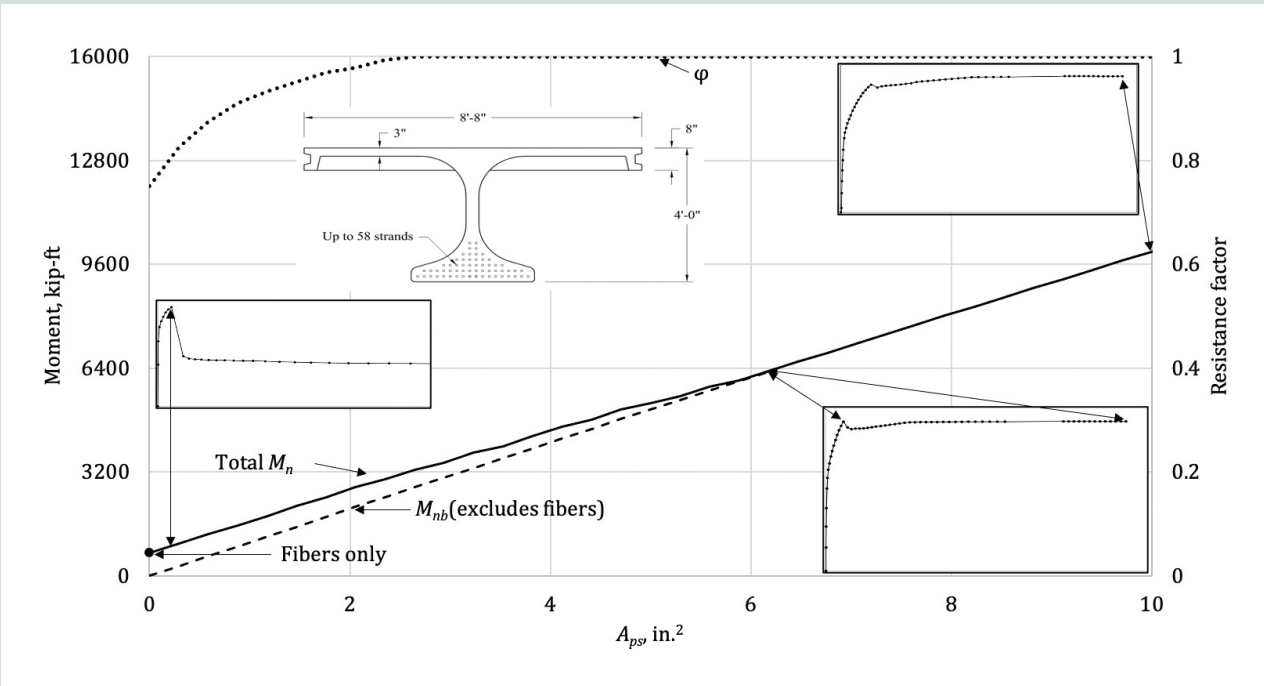

Figure 8. Nominal moment capacity of pretensioned section with the fiber contribution examined. Note: A_{ps} = area of prestressing steel; M_n = nominal flexural resistance; M_{nb} = nominal flexural resistance of flexural reinforcement only, ignoring fiber contribution. 1″ = 1 in. = 25.4 mm; 1′ = 1 ft = 0.305 m; 1 in.² = 645.2 mm²; 1 kip-ft = 1.356 kN-m.

when the section reaches ultimate strain in compression of 0.003. Note that 10 in.^{2} (6452 mm^2) of prestressing strand corresponds to about thirty-four 0.7 in. (17.8 mm) diameter strands or forty-six 0.6 in. (15.2 mm) diameter strands in the bottom flange. The figure also shows that the resistance factor, as recommended by Eq. (5), varies from as low as 0.75 for sections with fibers alone to as high as 1.0 for sections dominated by prestressing.

Contribution of fibers in nonprestressed UHPC members

Flexural behavior of the transverse direction of the top flange of a decked I-beam, the top flange of a box beam, or similar applications is best illustrated through the following three examples. First, consider the negative moment section at the face of the web in a decked I-beam with centerline-to-centerline spacing of 9 ft 6 in. (2.9 m). The total flange depth is 8 in. (203 mm). It consists of stems with an average width of 3.5 in. (89 mm) at a spacing of 24 in. (610 mm) and a top skin whose thickness is determined based on flexural demand, as subsequently described. It is desired to have no top bars and to depend totally on the fibers for the negative moment. One bottom Grade 100 (690 MPa) bar is desired to be placed in each stem. The size of the bar will be addressed later in this paper. The factored load positive moments at midspan between web centerlines and at the critical negative moment section, assumed to be 13 in. (330 mm) away from the centerline of the web, were determined according to the AASHTO LRFD specifications[20] to be 26.0 and 16.1 kip-ft (35.2 and 21.8 kN-m), respectively.

Figure 9 shows the moment-curvature relationship for the critical negative moment section for 2 in. (51 mm), 2½ in. (64 mm), and 3 in. (76 mm) top-skin thicknesses. After introduction of a resistance factor of 0.75, it appears from the figure that 2½ in. (64 mm) skin thickness is adequate.

Analysis for positive moment involves interaction between fibers and reinforcing bars. **Figure 10** shows the relationship between the moment capacity and the area of nonprestressed steel A_s provided at the bottom of the stem. For a specific A_{sfy} value, where f_y = yield strength of reinforcement, moment capacity is determined using a moment-curvature analysis such as that producing one curve in Fig. 9. Several points establish the total M_n line in Fig. 10. Also shown in Fig. 10 is a line representing the relationship when fibers are ignored and a point on the vertical axis when the bars are ignored. It can be seen that both the fibers and the steel bars contribute significantly to the nominal moment capacity of the positive moment section. Figure 10 also shows variability of the resistance factor ϕ from 0.75 to 0.90, depending on the share of the fibers' contribution to the total moment. The design is satisfactory when the factored moment M_u demand line intersects with the reduced capacity ϕM_n. The corresponding $A_s f_y$ is 42.6 kip (189.5 kN). Using no. 6 (19M) Grade 100 (690 MPa) steel, the design would require one bar per stem with a capacity of 44.0 kip (195.7 kN).

The third example is related to transverse design of the top slab of a ribbed slab panel proposed for use in multistory residential construction. A partial cross section of the product is shown in **Fig. 11**. The commercial product would be as wide

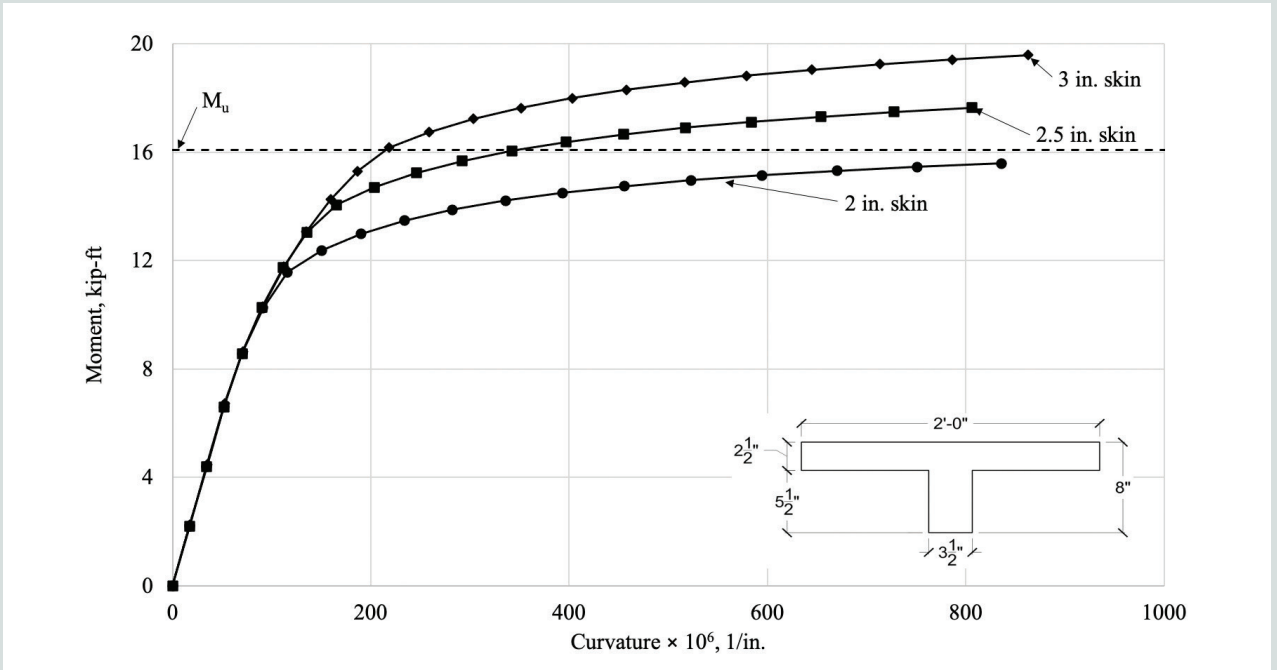

Figure 9. Determination of required top skin thickness for the decked I-beam shown in Fig. 12. Note: M_u = factored negative moment at the section. 1″ = 1 in. = 25.4 mm; 1′ = 1 ft = 0.305 m; 1 kip-ft = 1.356 kN-m.

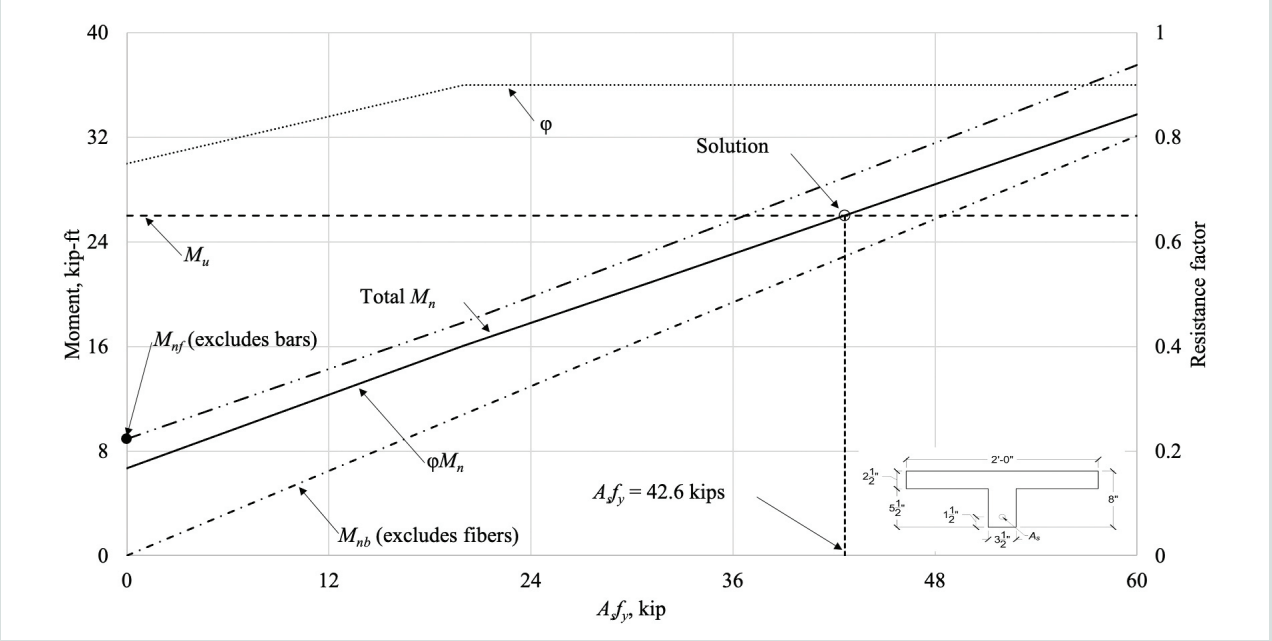

Figure 10. Determination of Grade 100 reinforcing bar size for positive moment resistance of the top flange of a decked I-beam. Note: A_s = area of nonprestressed tension reinforcement; f_y = specified minimum yield strength of reinforcement; M_n = nominal flexural resistance; M_{nb} = nominal flexural resistance of flexural reinforcement only, ignoring fiber contribution; M_{nf} = nominal flexural resistance of fibers only, ignoring flexural reinforcement; M_u = factored negative moment at the section. 1″ = 1 in. = 25.4 mm; 1′ = 1 ft = 0.305 m; 1 kip = 4.448 kN; 1 kip-ft = 1.356 kN-m.

as 12 ft (3.7 m), with four stems at 3 ft (0.9 m) spacing. The top slab is 1 in. (25 mm) thick and has a clear span of 26 in. (660 mm). Besides its own weight, the slab is subjected to a superimposed dead load of 40 lb/ft^2 (1.9 kN/m^2) and a live load of 100 lb/ft^2 (4.8 kN/m^2). The total factored load = 1.2(13 + 40) + 1.6(100) = 224 lb/ft^2 (10.7 kN/m^2). The factored load moment = 0.224 × (26/12)^2/10 = 0.11 kip-ft/ft (0.50 kN-m/m). Based on the moment curvature relationship, a nominal capacity of 0.32 kip-ft/ft (1.42 kN-m/m) has been determined. The reduced (design) capacity is 0.21 kip-ft/ft (0.93 kN-m/m), after accounting for a strength reduction factor for building products of $\phi = 0.65$. Thus, using the 1 in. (25 mm) thick slab without any reinforcing bars is adequate. A separate check of punching shear was also found to be satisfactory.

Additional influencing factors

In addition to the factors just discussed, flexural design is influenced by the strand bond to concrete, prestress losses, and camber estimates. The latter two are in turn influenced by creep and shrinkage estimates.

Strand bond At member end faces, the prestress is zero. It develops over a length equal to the transfer length at full force on the concrete section. The critical section due to prestress release is at a transfer length away from the member end face. Previous studies by Graybeal[33] and the PCI-UHPC phase I[1] report have indicated a superior bond of strands to the UHPC. Both reports indicate that the average transfer length is 20 strand diameters and the development length is 40 strand diameters. These values are good for UHPC exhibiting the type of tensile properties for the PCI-UHPC class specified in this paper. Flexural strength is affected by the development length, especially in short members. Also, if strand debonding at the ends is needed to control concrete stresses at release, a complete design would require checking stresses at a transfer length away from the end of debonding and strength analysis would require checking flexural strength at a development length away from the debonding point.

Creep, shrinkage, and prestress loss UHPC is known to exhibit significant autogenous shrinkage in the first few days after casting. There is no clear agreement in the literature on the amount of autogenous shrinkage or long-term creep and shrinkage of UHPC. Some research indicates that autogenous shrinkage in UHPC can be as high as 900 microstrains.[16,17] Once the UHPC is about 14 days of age, the specimen gets postcured, reducing the shrinkage to near zero. The average ultimate shrinkage for conventional concrete is about 480 microstrains, according to the AASHTO LRFD specifications.[20] The consensus is that once the member is cured with thermal postcuring within a couple of weeks of casting, both shrinkage and creep after postcuring appear to be minimal. Also, shrinkage-reducing-admixtures have been available if it is important to reduce or totally eliminate the autogenous shrinkage. The PCI-UHPC phase I[1] report has more details on this topic.

It is conservative to ignore the autogenous shrinkage when computing concrete stresses that are caused by the initial pre-

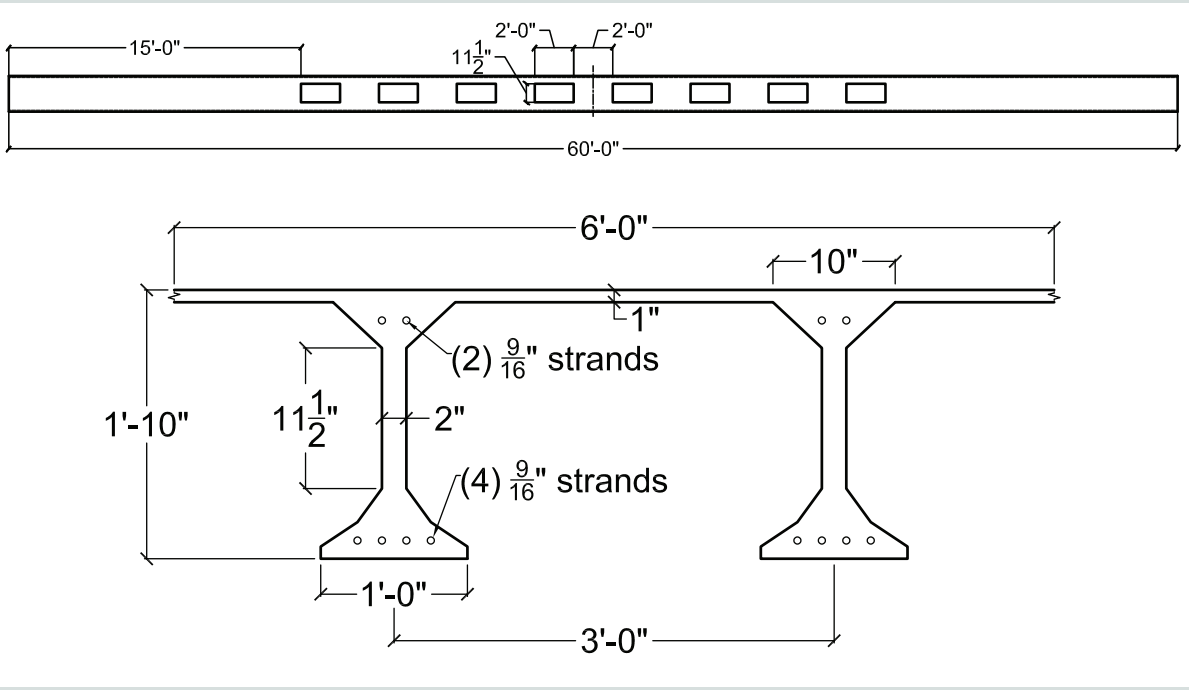

Figure 11. A 12 ft wide × 60 ft span optimized ultra-high-performance concrete voided slab for multistory residential applications. Note: 1″ = 1 in. = 25.4 mm; 1′ = 1 ft = 0.305 m.

stress and member weight. With this approach, the initial loss is low and the concrete stresses at release are high. The only drawback of this assumption is that the member is not fully stretched to its maximum span potential. Furthermore, the use of transformed section properties at release would eliminate any need to separately calculate initial prestress loss or initial prestress force after losses.

Creep in UHPC varies from 0.3 to as much as 1.2 compared with an average of 1.9 for conventional concrete. Estimated creep and shrinkage values may be used to estimate long-term prestress losses according to AASHTO LRFD specifications or other prediction methods; however, for calculations of concrete stresses at final conditions, it is reasonable to overestimate the total long-term losses in order to have a relatively low estimate of the effective prestress. In this stress check, it is currently recommended that the total prestress loss—including initial, creep, shrinkage, and strand relaxation losses—be assumed to equal 20% of the initial prestress (that is, 0.2 × 202.5 = 40.5 ksi [279 MPa]), resulting in effective prestress of 162 ksi (1117 MPa). Again, this is a conservative assumption and its potential drawback is the possible need for a few more strands than would be necessary with a lower long-term loss assumption. As more confidence is gained in time-dependent analysis with more-accurate creep and shrinkage estimates, these long-term estimates can be further refined and the span capacity of UHPC members extended.

Camber Initial camber is an elastic property that can be readily calculated using the theory of elasticity, as is explained, for example, in chapter 8 of the *PCI Bridge Design Manual*.[32]

Camber at erection is obtained from camber at release using creep multipliers. Again, given the uncertainty of the creep multipliers and the partial prestress loss at erection, simplifying assumptions will be used here. The goal is to have a flat or slightly cambered member if the member has an integral deck, such as decked I-beams. Sagging members are aesthetically undesirable by some owners.

Because of the high variability of long-term camber predictions, it is recommended that unbonded post-tensioned monostrands be employed at the top of the precast concrete member to provide for field adjustments for desired camber at the time of placement of asphalt overlays. In the example at the end of this paper, such a technique is demonstrated.

The deflection at erection due to the member weight combined with prestress is the deflection at release of prestress factored by a creep multiplier. The creep multiplier for effects of prestress and beam weight is $1+\psi_a$, where ψ_a = creep coefficient for loading applied immediately after transfer and sustained to time of erection. The prestress force used in this calculation should account for loss of prestress between release and erection.[32] Based on the phase I report,[1] the ultimate creep coefficient to time infinity for UHPC ψ_a when no special postcuring thermal treatment is applied is 1.2. The current formula for the time development factor k_{td} for creep, according to the AASHTO LRFD specifications[20] is as follows:

$$k_{td} = \frac{t}{12\left(\frac{100-4f'_{ci}}{f'_{ci}+20}\right)+t}$$

(AASHTO LRFD specifications 5.4.2.3.2-5)

where

t = time period between load application, prestress release in this case, and time at which creep effects are being assessed

When t is set as 120 days, k_{td} equals 0.83. Multiplying the ultimate creep coefficient (1.20) by the time development factor k_{td} results in a creep coefficient ψ_a of 1.0. The same formula can be used to estimate the camber at erection due to prestress. If the long-term prestress loss is assumed to be 20% of initial prestress, the deflection at erection due to prestress loss is adapted from the *PCI Bridge Design Manual*[32] Table 8.7.2-1 as the following:

$$\Delta_{pl} = \Delta_{pi} \times 0.20 \times (1 + 0.7 \times \psi_a) = 0.34\Delta_{pi} \quad (6)$$

where

Δ_{pl} = deflection (downward) due to prestress loss at erection

Δ_{pi} = initial camber (upward) due to prestress

Experimental verification

Precast, prestressed concrete decked I-beam

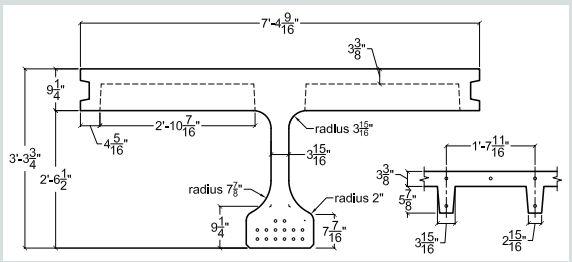

Figure 12. Cross section of the decked I-beam produced by FACCA Inc. Note: 1″ = 1 in. = 25.4 mm; 1′ = 1 ft = 0.305 m.

A 49.25 ft (15 m) long UHPC decked I-beam with a depth of 3 ft 3¾ in. (1 m) was produced by FACCA Inc. of Ruscom Station, ON, Canada, in early 2020. **Figure 12** shows the cross section of the beam. This beam is being used for an actual bridge designed by e.Construct structural engineering consultants in Omaha, Neb. The specimen includes an innovative design of a UHPC end wall to help reduce field activities. The 28-day compressive strength of the mixture that FACCA Inc. used was determined to be 23,300 psi (160 MPa) with flexural prism tests also significantly exceeding the minimum specified values.

This beam was tested for flexure. Testing was done at the North Carolina State University Constructed Facilities Lab. Because of the desire to test the beam to failure in shear, the flexural test only reached a load slightly above the design-factored load in accordance with Canadian standards.

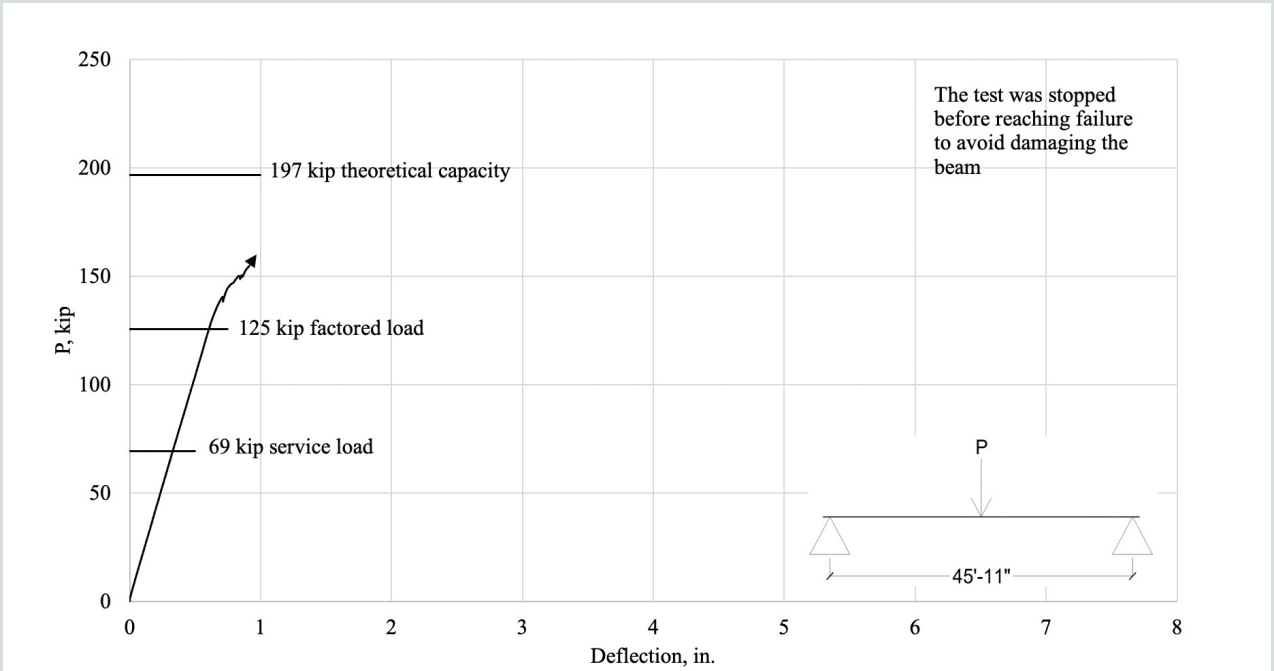

Figure 13. Load deflection curve of the decked I-beam. Note: P = applied load. 1″ = 1 in. = 25.4 mm; 1′ = 1 ft = 0.305 m; 1 kip = 4.448 kN.

Figure 13 shows the load-deflection curve. It can be seen that the beam remains linear elastic through the expected factored load of 125 kip (556 kN). Although no cracks were visible, the load-deflection curve suggests that the beam started to exhibit inelastic behavior.

Precast, prestressed concrete floor slab

A building floor slab system was designed to span 60 ft (18.3 m). **Figure 14** shows a sketch of a testing specimen. The actual product is expected to be as wide as 12 ft (3.7 m) and to have four ribs. The product is expected to carry residential loads and was designed for a 25 lb/ft^2 (1.2 kN/m^2) superimposed dead load and a 100 lb/ft^2 (4.8 kN/m^2) live load. The specimen was designed by e.Construct, produced by Tindall Corp., and tested at North Carolina State University. The stems had eight 10 × 24 in. (254 × 610 mm) blockouts to allow for passage and placement of utilities within the voids. Note that the top slab was only 1 in. (25 mm) thick, the stems were only 2 in. (51 mm) wide, and no shear or flexural reinforcement was used. The compressive strength was 16.3 ksi (112 MPa), which is less than the expected minimum of 18 ksi (124 MPa). The flexural testing results exceeded the minimum requirements for PCI-UHPC concrete. The floor slab was then tested by four-point bending using two different setups. The first test placed each ram 22.5 ft (6.9 m) from the closest support, which placed the point load very close to the midspan and directly above the stem opening. **Figure 15** shows the first test setup. The second test placed the rams 15 ft (4.6 m) from the closest support, at the edge of the first stem blockout.

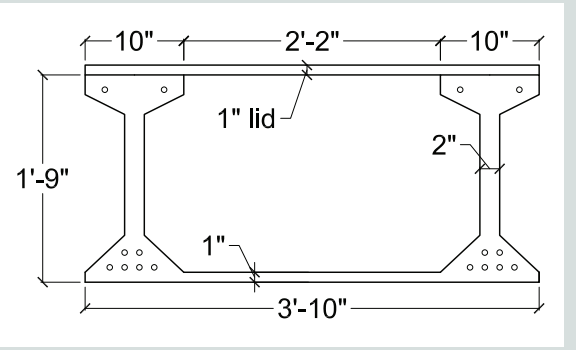

Figure 14. Cross section of building floor slab produced by Tindall Corp. Note: 1″ = 1 in. = 25.4 mm; 1′ = 1 ft = 0.305 m.

Figure 15. Test setup for the first flexure test of the floor slab.

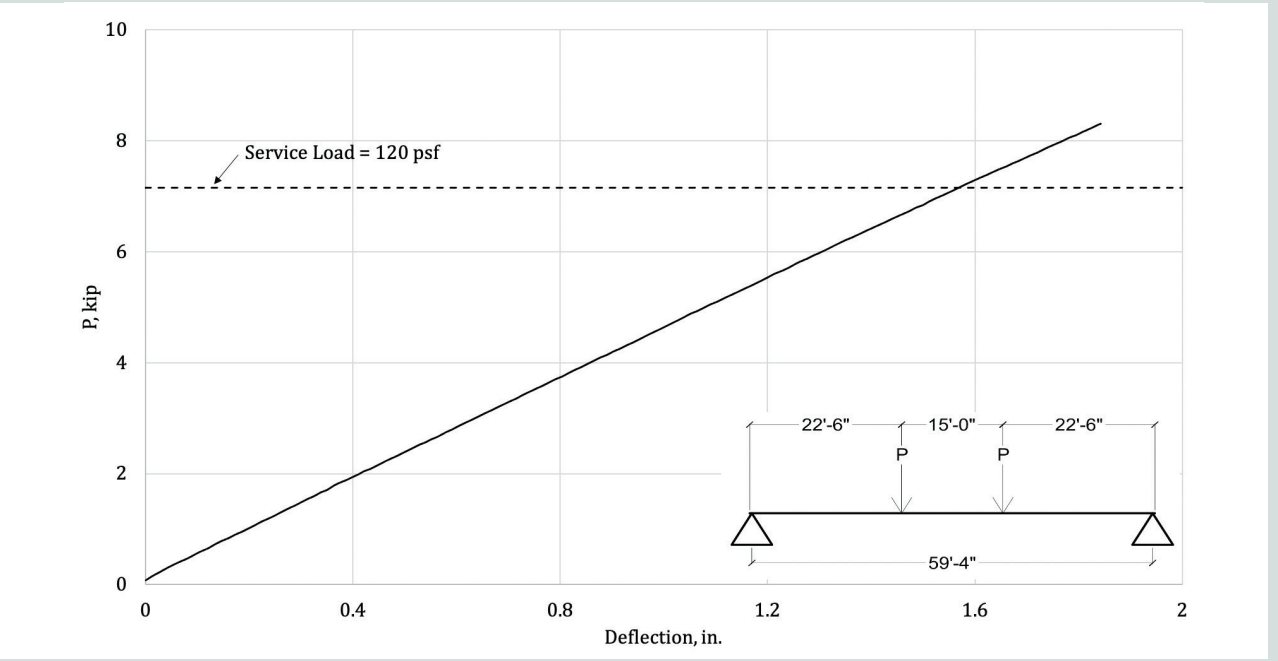

Figure 16. Load-deflection curve for the first flexure test. Note: *P* = applied load. 1″ = 1 in. = 25.4 mm; 1′ = 1 ft = 0.305 m; 1 kip = 4.448 kN; 1 psf = 47.880 Pa.

Figure 16 shows the load-deflection curve for one of the two tests. For the first test, it was observed that the stiffness was linear and no cracking at midspan was observed throughout the entire test. The specimen was loaded to an equivalent distributed load of 140 lb/ft^2 (6.7 kN/m^2). There was no relative slippage between the topping and the stems or between the strands and surrounding concrete. For the second test, the specimen was loaded to an equivalent distributed load of 200 lb/ft^2 (9.6 kN/m^2) before the lid slab started to lift off the beam (**Fig. 17**). This behavior showed that the connection of the lid slab to the first-stage component of the member should have been provided at a closer spacing than the 4 ft (1.2 m) provided. Although the lid started to lift off, no bottom flexural cracks were observed at midspan. Please note that this test was not primarily intended to test the structural product. It was done early in the research using somewhat imprecise wood forms for trial batching of UHPC at the Tindall facilities; however, the flexural and shear results (not discussed here) exceeded expectations.

Figure 17. Delamination of the top slab near failure. Note that no connecting interface bars were used.

Precast, prestressed concrete bridge box beam

A box beam was designed by e.Construct; produced by Standard Concrete Products (SCP) in Tampa, Fla.; and tested by the Florida Department of Transportation Marc Ansley Structures Lab in Tallahassee, Fla. The design was developed as an alternative UHPC product to a solid conventional concrete slab of the same height (1 ft 5 in. [0.4 m]) spanning 47 ft (14.3 m). SCP produced two beams: one with the conventional concrete design and the other with the UHPC design. **Figure 18** shows the details of the two designs. Note the near absence of reinforcing bars with the UHPC design and the high congestion of bars in the conventional design. The UHPC box beam had only 52% of the concrete of the conventional concrete product and less than 4% of the reinforcing bars. The same amount of prestressing was used for both beams to facilitate production of the two products in the same bed. The compressive strength of the UHPC box beam was 18.97 ksi (130.8 MPa), and the tensile properties exceeded minimum PCI-UHPC requirements. The UHPC box beam failed in flexure at approximately 148 kip (658.3 kN)

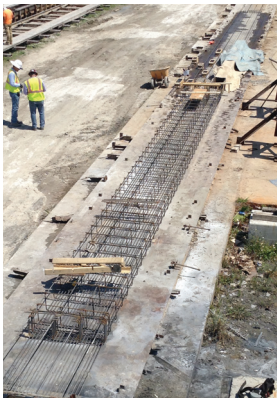

Ultra-high-performance concrete box slab

Conventional concrete solid slab

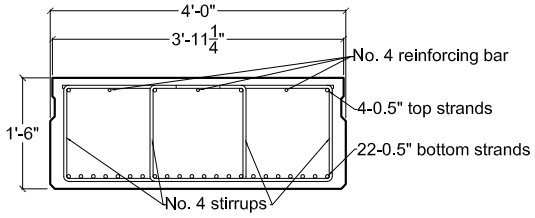

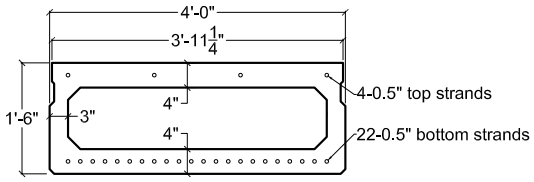

Figure 18 Ultra-high-performance concrete box slab compared with a conventional concrete solid slab. Both slabs were produced by Standard Concrete Products in Tampa, Fla., and tested at the Florida Department of Transportation Marc Ansley Structures Lab in Tallahassee, Fla. Note: no. 4 = 13M; 1″ = 1 in. = 25.4 mm; 1′ = 1 ft = 0.305 m.

Figure 19. Close-up of failure in flexure.

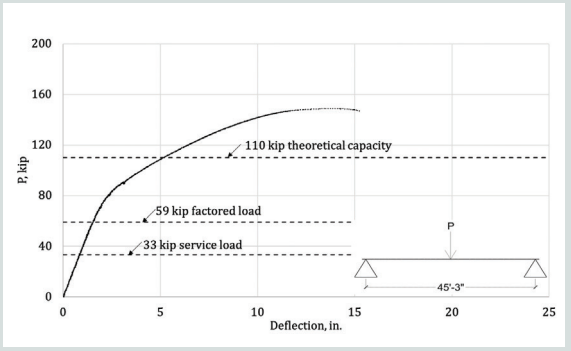

Figure 20. Load-deflection curve for the ultra-high-performance concrete box beam. Note: *P* = applied load. 1″ = 1 in. = 25.4 mm; 1′ = 1 ft = 0.305 m; 1 kip = 4.448 kN.

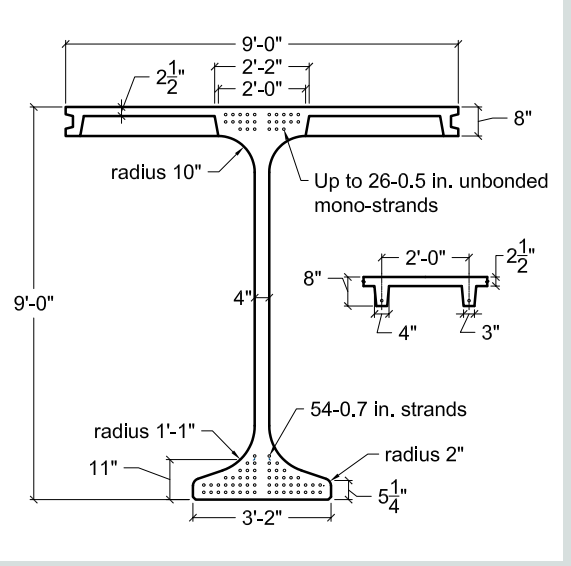

Figure 21. Dimensions of the decked I-beam cross section. Note: 1″ = 1 in. = 25.4 mm; 1′ = 1 ft = 0.305 m.

(**Fig. 19** and **20**). This compared to a required factored load of 59 kip (262.4 kN) and a theoretical ultimate load of 110 kip (489.3 kN), giving a 34.5% increase in actual capacity compared with predicted capacity. This wide margin could have been reduced in actual design by reducing the level of prestress, which was high to match that in the conventional concrete member. The UHPC box beam appeared to stay linear elastic past the factored load of 59 kip (263 kN) before cracking started to occur. A lesson learned in this project was to avoid using large concrete blocks to shim the expanded polystyrene foam blocks. Failure appeared to be triggered by the weakened section occupied by the shim blocks (Fig. 19).

Design example: 250 ft span decked I-beam

This design example demonstrates the design of a 250 ft (76.2 m) single-span UHPC decked I-beam bridge. This cross section was selected to demonstrate how structural engineers have a responsibility to optimize cross sections to take full advantage of the properties of PCI-UHPC. A more conventional approach to optimize the shape of an I-beam and to add conventional cast-in-place concrete deck is what most designers would think of implementing. Such a conventional approach results in relatively slow construction and in a deck with relatively low life expectancy and frequent maintenance expenses.

The design of a typical interior beam in flexure is considered. The total beam length was 252 ft (76.8 m) to allow for bearings. The total width of the bridge was 47 ft (14.3 m). Through iterations, the cross section of the beam was determined to have the dimensions shown in **Fig. 21**. Five girders were placed at a spacing of 9 ft 6 in. (2.9 m) to create the full bridge width of 47 ft (14 m) (**Fig. 22**). Because this system is suitable for accelerated bridge construction, a cast-in-place topping is not desired. Rather, a 3 in. (76 mm) asphalt overlay was used to provide a uniform riding surface and to accommodate the camber variability in this highly prestressed system. The prestressing of this beam required to resist highway loading per AASHTO LRFD specifications[20] was found through iterations to be 54 bonded pretensioned 0.7 in. (17.8 mm) diameter strands in the bottom flange and 14 unbonded post-tensioned 0.5 in. (12.7 mm) strands in the top flange (**Fig. 21**). The relatively large number of top unbonded strands allowed for high flexibility in adjusting the camber at the time the overlay was placed such that the final top surface profile met geometric requirements. Thus, although 26 positions of top strands were provided, the calculations presented in this example indicate that only 14 strands were needed to theoretically achieve a net camber at release of near zero. Because of the random variability of creep, shrinkage, and prestress losses and because it is uncertain at the time of design what the age of concrete would be at the time of erection and placement of the superimposed dead load, it would be prudent to provide the opportunity to post-tension more top strands than would be expected in design.

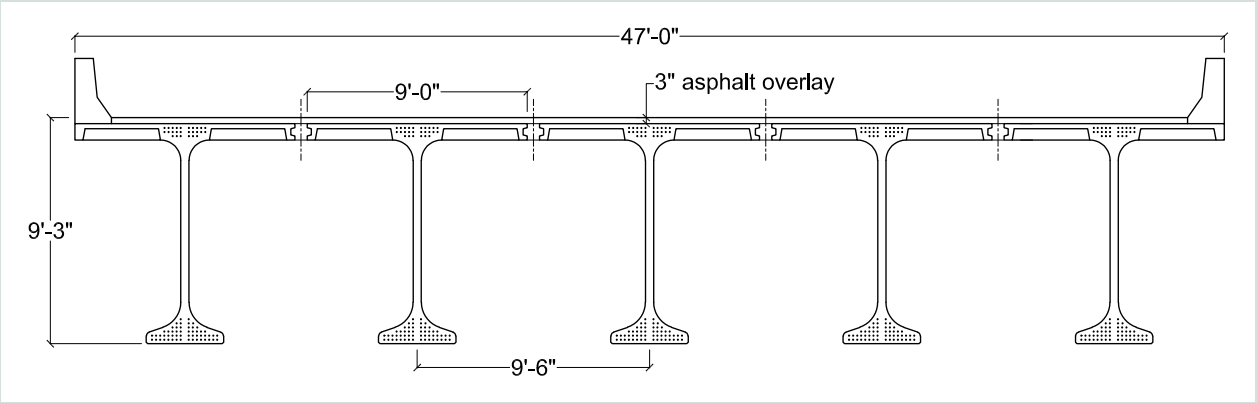

Figure 22. Bridge cross section. Note: 1″ = 1 in. = 25.4 mm; 1′ = 1 ft = 0.305 m.

The total top-flange depth was 8 in. (203 mm), of which 2½ in. (64 mm) was the top skin and the remaining 5½ in. (140 mm) was occupied by stems spaced at 24 in. (610 mm). An earlier section of this paper already detailed that the skin thickness is adequate to resist the applied loads without transverse reinforcement. Also, it has been shown that the reinforcement required at the bottom of the rib for positive moment resistance is no. 6 (19M) Grade 100 steel (690 MPa).

Loads

Beam weight (including ribs) = 1.35 kip/ft (19.7 kN/m); midspan moment = 10,546.9 kip-ft (14,299 kN-m)

Barriers = two of 0.3 kip/ft (4.4 kN/m) = 0.6 kip/ft (8.8 kN/m) = 0.12 kip/ft/beam (1.75 kN/m/beam); midspan moment = 937.5 kip-ft (1271 kN-m)

Longitudinal joint = 0.067 kip/ft (0.98 kN/m); midspan moment = 521.4 kip-ft (706.9 kN-m)

Wearing layer = 0.356 kip/ft (5.3 kN/m); midspan moment = 2781.3 kip-ft (3770.75 kN-m)

Live load: HL-93 per AASHTO LRFD specifications;[20] midspan moment = 4826.7 kip-ft (6543.8 kN-m) (truck plus impact) + 4300.0 kip-ft (5829.7 kN-m) (lane)

Concrete properties

Concrete unit weight = 0.155 kcf (2483 kg/m^3); modulus of elasticity of concrete at transfer E_{ci} = 5000 ksi (34,475 MPa); modulus of elasticity of concrete at service E_c = 6500 ksi (44,800 MPa)

The concrete is required to meet the compressive and tensile properties given for the PCI-UHPC class limits: Compressive strength = 10 ksi (69 MPa) at release and 18 ksi (124 MPa) at service. Tensile strength, per ASTM C1609,[4] at cracking = 1.5 ksi (10 MPa) and at peak load = 2 ksi (14 MPa), with the peak stress at least 125% of actual cracking stress and residual stress at deflection of $L/150$ = 75% of actual cracking stress.

Steel properties

Seven-wire 270 ksi (1860 MPa) prestressing strands were used. The areas of the 0.7 in. (17.8 mm) strand and 0.5 in. (12.7 mm) strand are 0.294 in.^{2} (189.7 mm^2) and 0.153 in.^{2} (98.7 mm^2), respectively. ASTM A1035[28] yield Grade 100 (690 MPa) reinforcing bars were used. Moduli of elasticity of the strands and bars are 28,500 and 29,000 ksi (196,508 and 199,955 MPa), respectively.

Strand pattern and initial prestress

The strands were placed as shown in **Fig. 21**. The centroid of the bottom strand group y_{bs} = 4.96 in. (126 mm). The initial tensioning force of the strands = 202.5 × 0.294 × 54 = 3215 kip (14,300 kN).

Creep, shrinkage, and prestress losses

The phase I report[1] discusses creep, shrinkage, and prestress losses in more detail than is provided here. For this paper, it was assumed that postcuring of the member at 194°F for 48 hours after prestress release will greatly control long-term creep and shrinkage. Further, it was assumed that initial prestress losses are automatically accounted for when transformed section properties are used and that the effective prestress due to initial loss plus creep, shrinkage, and relaxation effects is 80% of the initial prestress: 0.8 × 202.5 = 162 ksi (1117 MPa). This corresponds to a total initial plus long-term loss of 202.5 – 162 = 40.5 ksi (279 MPa). This value may seem to be high and not representative of the low creep and shrinkage values of UHPC; however, the cost may be a few more strands, which is manageable until more accurate information is developed. Elastic gains due to application of gravity loads (other than beam weight, which is already accounted for in the initial loss) are automatically accounted for when using transformed section properties.

Table 1. Section properties

Property	Gross section at release	Transformed section at release	Gross section at service	Transformed section at service
Area, in.^{2}	1193	1268	1255	1309
Moment of inertia, in.^{4}	2,270,256	2,488,610	2,381,306	2,554,034
Centroidal distance, in.	60.65	57.37	62.79	60.42

Note: 1 in. = 25.4 mm; 1 in.^{2} = 645.2 mm^2; 1 in.^{4} = 416,231 mm^4.

Table 1 lists the gross section properties of one beam at release and at service when the longitudinal joint becomes effective. The corresponding transformed section properties are also given. The bottom bonded strands are transformed to concrete using 28,500:5000 and 28,500:6500 modular ratios at prestress release and at service, respectively. The top strands are unbonded and do not contribute to the stiffness of the concrete.

Concrete stresses at transfer

Compression limit[20] = $0.60 f'_{ci}$ = 6 ksi (41.4 MPa)

Tension limit[1] = 0.75 ksi (5.2 MPa)

Stresses at transfer length section Stresses at a transfer length away from the end of the beam were checked against the limits. At this time, no top strands were tensioned. The actual beam length of 252 ft (76.8 m) was used for the span length due to expected camber and thus support at the beam ends.

Transfer length[1] = 20(strand diameter) = 20(0.7) = 14 in. = 1.167 ft (356 mm)

Beam weight moment M_g at transfer length x was determined from the following formula:

M_g = $0.5w_g(x)(L-x)$ = (0.5)(1.35)(1.167)(252 – 1.167) = 197.6 kip-ft (267.9 kN-m)

where

w_g = beam weight per unit length

Assuming the strands are stressed to 75% of the specified tensile strength, the prestressing force P_{pi} was calculated as:

P_{pi} = $(A_{ps})(0.75 \times f_{su})$ = (0.294)(54)(202.5) = 3215 kip (14,300 kN)

Stress in the top of beam f_t was computed as:

$$f_t = \frac{P_{pi}}{A_{ti}} - \frac{P_{pi}e_{ti}}{S_{tti}} + \frac{M_g}{S_{tti}} = \frac{3215}{1268} - \frac{3215(57.37-4.96)}{49{,}153} + \frac{197.6(12)}{49{,}153} = 2.54 - 3.43 + 0.05 = -0.84 \text{ ksi}$$

(5.8 MPa)

where

A_{ti} = area of transformed section at transfer

e_{ti} = eccentricity of strands with respect to the transformed section at transfer

S_{tti} = section modulus for the extreme top fiber of the transformed section at transfer

This is higher than the limit of -0.75 ksi (5.2 MPa). One option is to post-tension several of the top strands before the bottom strands are released. Another option is to debond some of the bottom strands. For this example, debond four strands in the bottom row and four in the second row. The resulting prestress is 2739 kip (12,183 kN), and the centroidal distance is 5.30 in. (134.6 mm). The corresponding stress is:

f_t = 2.18 – 2.94 + 0.05 = 0.71 < 0.75 ksi (4.9 < 5.2 MPa) (tension) OK

Similarly, the stress at the bottom fibers f_b were calculated from the formula:

$$f_b = \frac{P_{pi}}{A_{ti}} + \frac{P_{pi}e_{ti}}{S_{bti}} - \frac{M_g}{S_{bti}} = \frac{2739}{1257} + \frac{2739(57.85-5.30)}{42{,}448} - \frac{197.6(12)}{42{,}448} = 2.18 + 3.39 - 0.06 = 5.51 < 6 \text{ ksi}$$

(38 < 41.4 MPa) OK

where

S_{bti} = section modulus for the extreme bottom fiber of the transformed section at transfer

Concrete stresses at service loads

Stresses are checked for effective prestress plus full loads (Service I for top fibers and Service III for bottom fibers in the AASHTO LRFD specifications[20]) using transformed section properties at service. Assuming 20% prestress loss, the effective prestress $P_{pe} = 0.8P_{pi} = 0.8 \times 3215 = 2572$ kip (11,440 kN). The stress limit in compression = 0.6 = 0.6(18.0)

= 10.8 ksi (74.5 MPa), and the stress limit in tension, or first peak-tensile strength, = $-f_1$ = -1.00 ksi (7 MPa).

Using section properties given in Table 1, the top-fiber stresses were calculated using the section properties at service. This is an approximation. The prestress is initially applied to the initial transformed section, and the long-term losses should be applied to the section at service. It is conservative to assume the net effective force is applied at service. The beam weight is still applied at the time of the initial prestress. The forces due to the top unbonded post-tensioned strands are also considered. Camber analysis, shown later in this example, uses fourteen 0.5 in. (12.7 mm) top strands. The top strands are also applied to the transformed section at service, similar to the bottom strands. The joint is considered at service, and the section properties, including the transformed properties, account for this.

Top-fiber stresses f_{tg} were calculated as follows:

$$f_{tg} = \frac{P_{pe}}{A_{tf}} - \frac{P_{pe}e_{tf}}{S_{ttf}} + \frac{M_g}{S_{tti}} + \frac{M_{ws}+M_b+M_{LT}+M_{LL}}{S_{ttf}}$$

$$= \frac{2572}{1309} + \frac{347}{1309} - \frac{2572(55.46)}{53,679} - \frac{347(60.42-105.43)}{53,679}$$

$$+ \frac{11,068.3(12)}{49,155} + \frac{(2781.3+937.5+4826.7+4300.0)(12)}{53,679}$$

= 1.96 + 0.27 – 2.66 + 0.29 + 2.70 + 2.87 = 5.43 ksi

= 5.43 < 10.6 ksi (37.4 < 73 MPa) OK

where

A_{tf} = area of transformed section at service

e_{tf} = eccentricity of strands with respect to transformed section at service

S_{ttf} = section modulus for the extreme top fiber of the transformed section at final time

M_{ws} = unfactored bending moment due to the wearing surface (overlay)

M_b = unfactored bending moment due to the barrier

M_{LT} = unfactored bending moment due to the truck load with impact

M_{LL} = unfactored bending moment due to the lane load

Bottom fiber stresses f_b were calculated as follows:

$$f_b = \frac{P_{pe}}{A_{tf}} + \frac{P_{pe}e_{tf}}{S_{btf}} - \frac{M_g}{S_{bti}} + \frac{M_{ws}+M_b+0.8(M_{LT}+M_{LL})}{S_{btf}}$$

$$= \frac{2572}{1309} + \frac{347}{1309} + \frac{2572(55.46)}{42,271} + \frac{347(60.42-105.43)}{42,271}$$

$$- \frac{11,068.3(12)}{43,378} - \frac{[2781.3+937.5+0.8(4826.7+4300.0)(12)}{42,271}$$

= 1.96 + 0.27 + 3.37 – 0.37 – 3.06 – 3.13 = -0.96 ksi (6.6 MPa)

= 0.96 < 1.00 ksi (6.6 < 7 MPa) (tension) OK

where

S_{btf} = section modulus for the extreme bottom fiber of the transformed section at final time

Flexural strength

Total ultimate bending moment M_u for strength I, the basic load combination relating to the normal vehicular use of the bridge without wind, is as follows:

$$M_u = 1.25(DC) + 1.5(DW) + 1.75(LL + IM)$$

where

DC = dead load of structural components and nonstructural attachments

DW = dead load of wearing surfaces and utilities

LL = vehicular live load

IM = vehicular dynamic load allowance

The ultimate bending moment at midspan is as follows:

M_u = 1.25(10,546.9 + 521.4) + 1.25(937.5) + 1.5(2781.3) + 1.75(4826.7 + 4300.0) = 35,150.9 kip-ft (47,658 kN-m)

Determination of the flexural strength was performed iteratively using the online spreadsheet. The spreadsheet is comprehensive. It allows for including any number of rows of reinforcement, whether it is Grade 60 (420 MPa) steel bars or higher-grade bars. It allows for a row to be described anywhere within the cross section. Strands can be counted as individual rows or groups of strands represented by their centers. Again, strands near the top or near the bottom or anywhere in the section can be defined. The spreadsheet allows for inclusion of the tension contribution of the fibers. Therefore, the spreadsheet can be an effective parametric study tool at the disposal of the designer.

The spreadsheet was run a number of times for this example. Only one option is described in detail in the following discussion. This option included clusters of fifty-four 0.7 in. (17.8 mm) bottom strands at 4.96 in. (126 mm) from the bottom face and fourteen 0.5 in. (12.7 mm) top strands at 2.57 in. (65 mm) from the top face. The top strands in this particular run were assumed to be fully bonded. This inaccurate

assumption was only used to simplify consideration of this minor contribution to flexural strength. Using this assumption avoided the complications resulting from integrating unbonded strand strain over the full member length.

The spreadsheet employs iteration to reach convergence. Only the final iteration values are given in this paper to illustrate the process used in the spreadsheet. The process is to iterate for a value of the neutral axis depth that creates compatibility of strains and equilibrium of forces. Concrete strain is linear over member depth, and steel strain at any level is the same as that in the concrete at the same level. Strains are used with the stress-strain relationships to determine stress. Stress is integrated to calculated forces. Equilibrium of forces is reached when the sum of all forces equals zero. At this final iteration, the sum of moments due to individual forces about the top face of the section is the nominal flexural resistance M_n of the section. The nominal moment is multiplied by the resistance factor in the relevant code (the AASHTO LRFD specifications[20] for this example) to obtain the design (reduced) moment ϕM_n. The reduced design moment capacity should be not less than the factored load demand M_u.

The cross section for the I-beam example was first modeled as a series of concrete layers, each having a constant width. The distance to the neutral axis c = 4.76 in. (121 mm). The corresponding equivalent rectangular compression block depth $a = 0.65 \times c$ = 3.09 in. (78 mm). The strain diagram was determined by the neutral axis depth and the ultimate concrete strain, which was assumed to equal 0.003. Using the strain diagram, the strain at the top and bottom groups of strands and the depth at the concrete tensile strain limit of 0.005 were computed as shown in **Fig. 23**. The concrete compression block covered the top 2.5 in. (64 mm) layer, plus another 0.59 in. (15 mm) of the lower layer. Only a small fraction of the cross section, 12.70 in. (323 mm) deep, was considered effective in resisting forces. Of that depth, 4.76 in. (121 mm) were in compression. The tensile stress depth (12.70 – 4.76 = 7.94 in. [202 mm]) consisted of two zones: a triangular one and a rectangular one having a stress of 0.75 ksi (5.2 MPa). As seen by the triangular zone and its impact, the tension contribution of the fibers was so small it is generally not recommended to count it.

The top-zone strands were initially in tension, but that tension was reduced from the effective prestress as the loads were applied and the section deformed. This analysis showed that the 162 ksi (1117 MPa) effective prestress was reduced to 138 ksi (951 MPa) at ultimate flexure. As indicated previously, the strands were unbonded and the strain at midspan section should be a value between those computed here (162 and 138 ksi). Using the spreadsheet with the top strands ignored would have shown that they have insignificant contribution to the flexural strength because concrete in compression does not need help from these strands. The most significant tension force was the one in the bottom strands. It is shown that the strain there was greater than that required for the strands to reach their full design strength of 270 ksi (1862 MPa).

The forces were calculated from the stresses and the corresponding areas. Their values are shown in **Fig. 23**. It is important at this time to check equilibrium. The sum of forces = -4361 – 364 + 143 + 4287 + 295 = 0. Taking moments of these forces about the top face of the section yields M_n = 36,422 kip-ft (49,382 kN-m). Because the strain at the extreme tensile layer of steel was much higher than that required for ductile behavior and because the member being designed is a bridge member, the resistance factor ϕ = 1.00. Thus, ϕM_n = 36,422 kip-ft (49,382 kN-m) > M_u = 35,151 kip-ft

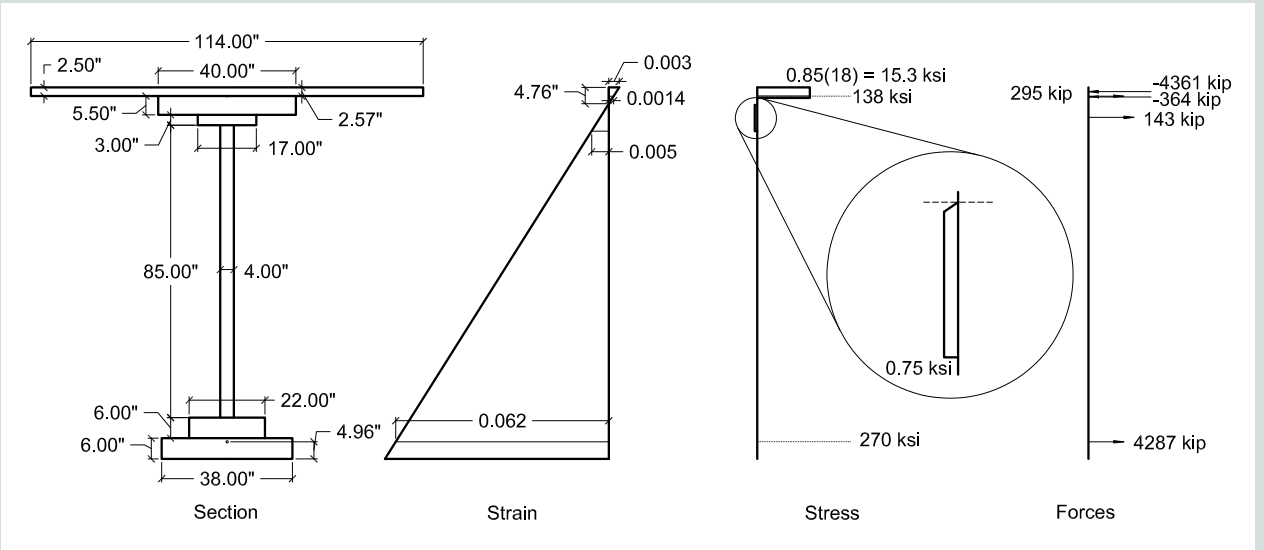

Figure 23. Cross-section modeling and output of the strain compatibility spreadsheet. Note: 1″ = 1 in. = 25.4 mm; 1 kip = 4.448 kN; 1 ksi = 6.895 MPa.

(47,656 kN-m). A parametric study was conducted to investigate the influence of various assumptions that could be used in the analysis.

When the contribution of fibers was ignored, M_n = 36,366 kip-ft (49,306 kN-m). When the strands were input in individual layers and fibers were ignored, the resulting M_n = 36,367 kip-ft (49,307 kN-m). When top strands and fibers were both ignored, M_n = 36,367 kip-ft (49,307 kN-m). Thus, one could obtain the capacity within less than 0.5% by lumping all bottom strands into one point, ignoring the top strands, and ignoring the fibers. These observations, though common, cannot be generalized. The results will vary with cross-section shape, depth, and level of prestress.

Camber and deflection

Camber was determined based on the contribution of the bottom strands, and deflection was based on the beam weight and the top post-tensioning of fourteen 0.5 in. (12.7 mm) strands. Camber at release was determined as follows:

Elastic deflection due to the girder weight is calculated as follows:

$$\Delta_g = \frac{5w_gL^4}{384E_{ci}I_{ti}} = \frac{5(1.35)(250)^4}{384(5000)(2,488,610)}(12)^3$$
$$= 9.54 \text{ in. (242 mm) (down)}$$

where

I_{ti} = moment of inertia of the transformed section at transfer

Net camber due to the bottom and top strands is calculated as follows:

$$\Delta_{pi} = \frac{P_{pi}e_{ti}L^2}{8E_{ci}I_{ti}} = \frac{(3215)(52.41)(250)^2}{8(5000)(2,488,610)}(12)^2$$
$$+\frac{(434)(-48.06)(250)^2}{8(5000)(2,488,610)}(12)^2$$
$$= 13.34 \text{ in. (339 mm) (up)}$$

Following the recommendations shown earlier for the creep coefficient and long-term prestress loss, the multipliers recommended in the *PCI Bridge Design Manual*[32] were used. The net camber due to prestress of top and bottom strands was multiplied by $(1 + \psi_a)$, where the creep coefficient for loading applied immediately after transfer and strains measured at time of erection ψ_a was determined to be 1 at an assumed time of erection of 120 days. The deflection due to the self-weight of the beam was also multiplied by the same factor. The prestress loss was assumed to be 20% of the initial prestress and the creep multiplier is $1 + \chi\psi_a$, where χ is the aging coefficient to account for gradual development of prestress loss. The aging coefficient may be taken as 0.7 as recommended in the *PCI Bridge Design Manual*.[32] Thus, the factor of 0.2(1 + 0.7) = 0.34 applied to the initial camber due to prestress was used to determine the long-term deflection due to prestress loss at the time of erection. The components of camber/deflection at erection were as follows:

Camber due to prestress = 26.68 in. (678 mm)

Deflection due to prestress loss = -4.54 in. (115 mm)

Deflection due to self-weight = -19.08 in. (485 mm)

Deflection due to superimposed dead load is calculated as follows:

$$\Delta_{SIDL} = \frac{5w_gL^4}{384E_cI_{tf}} = -\frac{5(0.54)(250)^4}{384(6500)(2,554,034)}(12)^3$$
$$= -2.86 \text{ in. (73 mm)}$$

where

I_{tf} = moment of inertia of the transformed section at service

This gives a final camber of 0.2 in. (5 mm) (upward). This amount of camber is generally considered to be tolerable since the beam is near flat due to all the prestress and dead load effects.

Conclusion

This paper presents recommendations for simplified, yet rigorous, analysis of the critical cross sections in UHPC flexural members for conditions at release of prestress and at final conditions. It covers both service load analysis and factored load analysis. It is recommended for use in bridge products with AASHTO LRFD specifications[20] load and resistance factors and in building products with ACI 318[5] load and resistance factors.

Designers may use the recommendations in this paper for design with any UHPC mixture, whether proprietary or locally mixed by precasters, as long as the mixture meets the specific conditions specified for the PCI-sponsored research project on UHPC and described in the phase I report.[1] Specifically, concrete compressive strength, per ASTM C39,[3] is specified as 10 ksi (69 MPa) at prestress release and 18 ksi (124 MPa) at service. Concrete tensile properties, per ASTM C1609,[4] are specified as follows:

- Cracking strength equals 1.5 ksi (10 MPa).
- Stress at peak load equals 2.0 ksi (14 MPa).
- The strain-hardening requirement is that peak stress must be at least 125% of cracking stress.
- The ductility requirement is that residual stress at a deflection of span/150 is at least 75% of cracking stress.

If the designer wishes to use the proposed recommendations for materials that have lower strength, strain hardening, or ductility than the PCI-UHPC mixture, adjustments must be made to the design criteria.

The properties of the PCI-UHPC mixture, especially strain hardening and ductility, allow for the possibility of very thin members. For example, floor slabs in buildings can be as thin as 1 in. (25.4 mm) without a need for continuous reinforcement. Webs in 9 ft (2.7 m) deep bridge I-beams can be as thin as 4 in. (102 mm) without a need for stirrups.

Through the inverse analysis performed in this paper and compared with previous research and international codes, the flexural prism analysis given by ASTM C1609[4] for fiber-reinforced concrete can be converted to a stress limit to be used in nonlinear moment-curvature analysis up to member failure. The inverse analysis indicates that one can assume a bilinear stress-strain diagram in tension with the peak stress specified as 0.75 ksi (5.2 MPa). A conservative recommendation at this time is to limit the fiber tensile strength contribution to concrete in flexure to that corresponding to strain between zero and 0.005. Beyond that strain, the fiber tensile strength is assumed to drop to zero.

It has been found through parametric analysis that the contribution of fibers to the peak moment in a cross section is a function of the geometry of the cross section and whether it is prestressed or conventionally reinforced. For prestressed members with typical levels of prestressing, fiber contribution to flexural strength is negligible. For conventionally reinforced tee beam sections, the fibers may be the only reinforcement needed when the flange is in tension. The designer always has the option to include the fiber contribution using the workbook developed by the authors and offered as a design tool in the online appendix.

It has been observed in this research and in previous studies that UHPC with continuous conventional reinforcing bars may have two peaks in the moment-curvature diagram. The first peak takes place at the fiber tensile capacity, and the second peak may develop with yielding of the reinforcing bar. To provide the required capacity, it is recommended to perform the moment-curvature analysis to capture the first peak when fibers are combined with reinforcing bars.

The model recommended in this paper for a compressive stress-strain diagram used for design of prestressed concrete sections is the same as the model that has been used for several decades. Namely, assume equivalent rectangular stress block at a stress of $0.85f_c'$ over a compression block depth $a = \beta_1 \times c$ where β_1 is 0.65 for concrete strength ≥ 8 ksi (55.2 MPa). For conventionally reinforced members, in addition to the strength calculated at the ultimate strain for prestressed members, it is recommended to develop the moment-curvature relationship using bilinear tensile stress and linear compressive stress bounded at $0.85f_c'$ and the corresponding strain of 0.00235. This approach will capture potentially two flexural strength peaks in a member reinforced with two types of tension-resisting elements, fibers, and continuous reinforcement (strands and/or bars).

Numerical examples of the cross sections of different configurations were given in this paper to illustrate the various effects discussed. Experimental results were compared with analysis for a number of product shapes and applications. It was shown that the recommendations consistently give conservative results while preserving the cost effectiveness of optimized cross-section dimensions. For example, it was shown that the 1 in. (25 mm) thick floor slab was able to resist an equivalent loading of 200 lb/ft^2 (9.6 kN/m^2). The box-beam experiments indicated that the actual capacity was almost 35% higher than the capacity predicted by the proposed design procedure.

An example of an interior beam of a bridge with a span of 250 ft (76.2 m) and a width of 47 ft (14.3 m) was given to illustrate the design procedure. No single-piece precast, prestressed concrete I-girder that can span 250 ft has even been built in the United States. The light weight resulting from optimized use of high-performance materials allows for this goal to be achieved. Large-diameter strands and Grade 100 (690 MPa) ASTM A1035[28] bars are significant contributors to this futuristic design. Only five beams are needed to complete the superstructure, and the absence of cast-in-place concrete would help with accelerated bridge construction.

Acknowledgments

The authors appreciate the financial support of PCI and the in-kind contributions of e.Construct and other participating partners, including Wiss, Janney, Elstner Associates; University of Nebraska–Lincoln; North Carolina State University; the Florida Department of Transportation Structures Laboratory; Louisiana Tech University; and Ohio State University. Six major precast concrete companies contributed their knowledge and financial resources to make the PCI project successful. They are Coreslab Structures in Omaha, Neb.; Standard Concrete Products; Metromont Corp.; Tindall Corp.; Concrete Technology Corp.; and FACCA Inc. Support of Jackie Voo of Dura Co. in Malaysia is gratefully acknowledged.

References

1. e.Construct USA LLC. 2020. "Implementation of Ultra-high-performance Concrete in Long-Span Precast Pretensioned Elements for Concrete Buildings and Bridges: Phase I Report." Chicago, IL: PCI. https://www.pci.org/PCI_Docs/Members_Only/Research%20Reports/Material/IMPLEM.pdf.

2. ASTM International. 2017. *ASTM Standard C1856: Standard Practice for Fabricating and Testing Specimens of Ultra-high Performance Concrete*. West Conshohocken, PA: ASTM International. doi:10.1520/C1856_C1856M-17.

3. ASTM International. 2020. *ASTM Standard C39: Standard Test Method for Compressive Strength of Cylindri-*

cal Concrete Specimens. West Conshohocken, PA: ASTM International. doi:10.1520/C0039_C0039M-20.

4. ASTM International. 2019. *ASTM Standard C1609: Standard Test Method for Flexural Performance of Fiber Reinforced Concrete (Using Beam with Third-Point Loading)*. West Conshohocken, PA: ASTM International. doi:10.1520/C1609_C1609M-12.

5. ACI (American Concrete Institute) Committee 318. 2019. *Building Code Requirements for Structural Concrete (ACI 318-19) and Commentary (ACI 318R-19)*. Farmington Hills, MI: ACI.

6. ASTM International. 2019. *ASTM Standard C1202-19: Standard Test Method for Electrical Indication of Concrete's Ability to Resist Chloride Ion Penetration*. West Conshohocken, PA: ASTM International. doi:10.1520/C1202-19.

7. Reineck, K. H., and B. Frettlöhr. 2010. "Test on Scale Effect of UHPFRC Under Bending and Axial Forces." Third *fib* International Congress, Washington, DC.

8. Graybeal, B., and F. Baby. 2013. "Direct Tension Test Method for UHPFRC." *ACI Materials Journal* 110 (2): 177–186.

9. López, J., P. Serna, J. Navarro-Gregori, and T. Camacho. 2015. "An Inverse Analysis Method Based on Deflection to Curvature Transformation to Determine the Tensile Properties of UHPFRC." *Materials and Structures* 48 (11): 3703–3718.

10. AFNOR (Association Française de Normalisation). 2016. *National Addition to Eurocode 2—Design of Concrete Structures: Specific Rules for Ultra-High-Performance Fibre-Reinforced Concrete (UHPFRC)*. NF P 18-710. Paris, France: AFNOR.

11. SIA (Swiss Society of Engineers and Architects). 2016. "SIA Standard 2052: Ultra-high Performance Fiber Reinforced Cement-Based Composites (UHPFRC)." (English translation of the technical leaflet SIA 2052 with adaptations, MCS-EPFL). Lausanne, Switzerland: SIA.

12. DAfStb (German Committee for Structural Concrete). 2017. *Guideline: Ultra-high Performance Concrete.* Berlin, Germany: DAfStb.

13. CSA (Canadian Standards Association). 2019. "Annex 8.1: Fibre Reinforced Concrete." In *CSA S6-19: Canadian Highway Bridge Design Code.* Mississauga, ON, Canada: CSA.

14. Gowripalan, N., and R. I. Gilbert. 2000. *Design Guidelines for Ductal Prestressed Concrete Beams.* Sydney, Australia: VSL.

15. Graybeal, B. 2008. "Flexural Behavior of an Ultra-High-Performance Concrete I-Girder." *Journal of Bridge Engineering* 13(6): 602–610.

16. Graybeal, B. 2006. "Structural Behavior of Ultra-high Performance Concrete Prestressed I-Girders." Federal Highway Administration (FHWA) report FHWA-HRT-06-115. McLean, VA: FHWA.

17. Vande Voort, T. L., M. Suleiman, and S. Sritharan. 2008. "Design and Performance Verification of UHPC Piles for Deep Foundations." IHRB project TR-558. Ames, IA: Center for Transportation Research and Education, Iowa State University.

18. Fehling, E., and T. Leutbecher. 2011. "Design of UHPC Members." In *Ninth Munich Construction Materials Seminar, UHPC: Materials, Design, Practice,* pp. 24–25. Munich, Germany: FördervereinBaustoff-Forschung e.V.

19. Naaman, A. E. 2017. *Fiber Reinforced Cement and Concrete Composites*. Sarasota, FL: Techno Press 3000.

20. AASHTO (American Association of State Highway and Transportation Officials). 2020. *AASHTO LRFD Bridge Design Specifications*, 9th ed. Washington, DC: AASHTO.

21. JSCE (Japan Society of Civil Engineers). 2008. *Recommendations for Design and Construction of High-Performance Fiber Reinforced Cement Composites with Multiple Fine Cracks (HPFRCC).* Concrete Engineering Series 82. Tokyo, Japan: JSCE.

22. KCI (Korea Concrete Institute). 2012. *Guidelines for K-UHPC Structural Design.* Seoul, South Korea: KCI.

23. Rizkalla, S., A. Mirmiran, P. Zia, H. Russell, and R. Mast. 2007. *Application of the LRFD Bridge Design Specifications to High-Strength Structural Concrete: Flexure and Compression Provisions*. NCHRP (National Cooperative Highway Research Project) report 595. Washington, DC: Transportation Research Board.

24. López, J., P. Serna, J. Navarro-Gregori, and H. Coll. 2016. "A Simplified Five-Point Inverse Analysis Method to Determine the Tensile Properties of UHPFRC from Unnotched Four-Point Bending Tests." *Composites Part B: Engineering* 91: 189–204.

25. Graybeal, B. 2006. *Material Property Characterization of Ultra-high Performance Concrete*. FHWA-HRT-06-103. McLean, VA: FHWA.

26. Naaman, A. E., and R. H. Reinhardt. 2006. "Proposed Classification of HPFRC Composites Based on Their Tensile Response." *Materials and Structures* 39: 547–555. doi:10.1617/s11527-006-9103-2.

27. ASTM International. 2020. *ASTM A615/A615M-20: Standard Specification for Deformed and Plain Carbon-Steel Bars for Concrete Reinforcement*. West Conshohocken, PA: ASTM International. doi:10.1520/A0615_A0615M-20.

28. ASTM International. 2019. *ASTM Standard A1035: Standard Specification for Deformed and Plain, Low-Carbon, Chromium, Steel Bars for Concrete Reinforcement*. West Conshohocken, PA: ASTM International. doi:10.1520/A1035_A1035-19.

29. ACI Innovation Task Group 6. 2010. *Design Guide for the Use of ASTM A1035/A1035M Grade 100 (690) Steel Bars for Structural Concrete*. ACI ITG-6R-10. Farmington Hills, MI: ACI.

30. Devalapura, R. K., and M. K. Tadros. 1992. "Stress-Strain Modeling of 270 ksi Low-Relaxation Prestressing Strands." *PCI Journal* 37 (2): 100–106.

31. ASTM International. 2018. *ASTM Standard A416: Standard Specification for Low-Relaxation, Seven-Wire Steel Strand for Prestressed Concrete*. West Conshohocken, PA: ASTM International. doi:10.1520/A0416_A0416-18.

32. PCI. 2014. *PCI Bridge Design Manual*. 3rd ed. Chicago, IL: PCI.

33. Graybeal, B. 2014. "Splice Length of Prestressing Strands in Field-Cast UHPC Connections." *Materials and Structures* 48 (6): 9.

Notation

a = depth of the equivalent compression stress block

A_{ps} = area of prestressing steel

A_s = area of nonprestressed tension reinforcement

A_{tf} = area of transformed section at service

A_{ti} = area of transformed section at transfer

c = distance from the extreme compression fiber to the neutral axis

d_s = distance from extreme compression fiber to the centroid of the nonprestressed tensile reinforcement measured along the centerline of the web

DC = dead load of structural components and nonstructural attachments

DW = dead load of wearing surfaces and utilities

e_{tf} = eccentricity of strands with respect to the transformed section at service

e_{ti} = eccentricity of strands with respect to the transformed section at transfer

E = modulus of elasticity

E_c = modulus of elasticity of concrete

E_{ci} = modulus of elasticity of concrete at transfer

E_s = modulus of elasticity of steel reinforcement

f_b = concrete tensile stress at bottom fiber of the beam

f'_c = compressive strength of concrete for use in design

f'_{ci} = required concrete compressive strength at transfer

f_{fc} = first-peak flexural stress using linear stress analysis in accordance with ASTM C1609

f_{fe} = equivalent bilinear strength to the linear peak stress obtained by ASTM C1609

f_{py} = yield strength of prestressing steel

f_s = allowable stress in steel

f_{su} = specified tensile strength of steel

f_t = the tensile stress corresponding to certain loads during uniaxial tensile tests; top-fiber normal stresses due to prestress and beam weight at transfer

f_{tc} = first-peak (cracking) stress using uniaxial tensile tests

f_{tg} = top-fiber normal stresses due to prestress and external loads under the service limit state

f_y = specified minimum yield strength of reinforcement

f_1 = specified first-peak tensile strength for use in design

h = overall thickness or depth of a member

I = moment of inertia

I_{tf} = moment of inertia of the transformed section at service

I_{ti} = moment of inertia of the transformed section at transfer

IM = vehicular dynamic load allowance

k_{td} = time development factor

K = curve-fitting constant

L = span length of the prism during the flexural test in accordance with ASTM C1609; span length

L_f = fiber length

LL = vehicular live load

M_b = unfactored bending moment due to the barrier

M_g = unfactored bending moment due to the beam self-weight

M_n = nominal flexural resistance

M_{nb} = nominal flexural resistance of flexural reinforcement only, ignoring fiber contribution

M_{nf} = nominal flexural resistance of fibers only, ignoring flexural reinforcement

M_u = factored moment at the section

M_{ws} = unfactored bending moment due to the wearing surface (overlay)

M_{LL} = unfactored bending moment due to the lane load

M_{LT} = unfactored bending moment due to the truck load with impact

P = applied load

P_{pe} = total prestressing force after all losses

P_{pi} = total prestressing force before transfer

Q = curve-fitting constant

R = curve-fitting constant

S_{btf} = section modulus for the extreme bottom fiber of the transformed section at final time

S_{bti} = section modulus for the extreme bottom fiber of the transformed section at transfer

S_{ttf} = section modulus for the extreme top fiber of the transformed section at final time

S_{tti} = section modulus for the extreme top fiber of the transformed section at transfer

t = time period between load application and time at which creep effects are being assessed

w = load per unit length

w_g = beam weight per unit length

x = transfer length (20 strand diameters)

y_{bs} = centroid of bottom strand group

β_1 = stress factor of compression block

Δ_g = deflection due to the beam weight

Δ_{pi} = initial camber due to prestress and post-tension forces

Δ_{pl} = deflection due to prestress loss from long-term effects

Δ_{SIDL} = deflection due to superimposed dead load at final time

ε_c = strain of concrete in extreme compressed fiber

ε_{cu} = failure strain of concrete in compression

ε_m = compressive strain at peak compressive stress

ε_s = strain in the reinforcement

ε_{tu} = design failure strain of concrete in tension

ϕ = resistance factor for moment

ϕ_b = resistance factor in accordance with the respective code based on tension-controlled, compression-controlled, or transition conditions with fiber contribution ignored

ϕ_{cc} = resistance for compression-controlled members

ϕ_{tc} = resistance for tension-controlled members

ϕ = Bazant's aging coefficient

ϕ_a = creep coefficient for loading applied immediately after transfer and sustained to time of erection

About the authors

Chungwook Sim, PhD, is an assistant professor in the Department of Civil and Environmental Engineering at the University of Nebraska–Lincoln.

Maher Tadros, PhD, PE, is a founding principal of e.Construct USA LLC. He is a distinguished emeritus professor and a PCI Medal of Honor recipient.

David Gee is a structural engineer with e.Construct, specializing in ultra-high-performance concrete (UHPC) and bridge design.

Micheal Asaad, PhD, PE, is a senior structural engineer with e. Construct, specializing in UHPC and bridge engineering. He has received awards for contributions to the American Concrete Institute and ASTM International.

Abstract

Ultra-high-performance concrete (UHPC) is a special concrete mixture with outstanding mechanical and durability characteristics. It is a mixture of portland cement, supplementary cementitious materials, sand, and high-strength, high-aspect-ratio microfibers. In this paper, the authors propose flexural design guidelines for precast, prestressed concrete members made with concrete mixtures developed by precasters to meet minimum specific characteristics qualifying it to be called PCI-UHPC. Minimum specified cylinder strength is 10 ksi (69 MPa) at prestress release and 18 ksi (124 MPa) at the time the member is placed in service, typically 28 days. Minimum flexural cracking and tensile strengths of 1.5 and 2 ksi (10 and 14 MPa), respectively, according to ASTM C1609 testing specifications are required. In addition, strain-hardening and ductility requirements are specified. Tensile properties are shown to be more important for structural optimization than cylinder strength. Both building and bridge products are considered because the paper is focused on capacity rather than demand. Both service limit state and strength limit state are covered. When the contribution of fibers to capacity should be included and when they may be ignored is shown. It is further shown that the traditional equivalent rectangular stress block in compression can still be used to produce satisfactory results in prestressed concrete members. A spreadsheet workbook is offered online as a design tool. It is valid for multilayers of concrete of different strengths, rows of reinforcing bars of different grades, and prestressing strands. It produces moment-curvature diagrams and flexural capacity at ultimate strain. A fully worked-out example of a 250 ft (76.2 m) span decked I-beam of optimized shape is given.

Keywords

ABC; accelerated bridge construction; camber of UHPC; creep of UHPC; decked I-beam; flexural design; flexural strength; high-strength fiber; I-beam; inverse analysis; long-span bridge beam; moment-curvature relationship; optimized structural products; precast, prestressed concrete beams; service limit state, steel fiber; strength limit state; UHPC; ultra-high-performance-concrete.

Review policy

This paper was reviewed in accordance with the Precast/Prestressed Concrete Institute's peer-review process.

Reader comments

Please address any reader comments to *PCI Journal* editor-in-chief Tom Klemens at tklemens@pci.org or Precast/Prestressed Concrete Institute, c/o *PCI Journal*, 8770 W. Bryn Mawr Ave., Suite 1150, Chicago, IL 60631.